CIRCADIAN CLOCK DISRUPTION IMPROVES THE EFFICACY OF CHEMOTHERAPY THROUGH p73-MEDIATED APOPTOSIS

Jin Hyup Lee

A dissertation submitted to the faculty of the University of North Carolina at Chapel Hill in partial fulfillment of the requirements for the degree of Doctor of Philosophy in the Department of Biochemistry and Biophysics.

Chapel Hill
2011

Approved by:

Aziz Sancar

Leslie Parise

Yue Xiong

Mohanish Deshmukh

Channing Der

ABSTRACT

Jin Hyup Lee: Circadian clock disruption improves the efficacy of chemotherapy through p73-mediated apoptosis
(Under the direction of Aziz Sancar)

The circadian clock in mammalian organisms is generated by a transcription-translation feedback loop (TTFL) which controls many biochemical pathways at the cellular level and physiology and behavior at the organismal level. Cryptochrome (Cry) is a key protein in the negative arm of the TTFL. It has been found that Cry mutation in cells with p53-null genotype increased their sensitivity to apoptosis by genotoxic agents. Here, I show that this increased sensitivity is due to upregulation of the p53 gene family member p73 in response to DNA damage. As a consequence, when tumors arising from oncogenic Ras-transformed $p53^{-/-}$ and $p53^{-/-}Cry1^{-/-}Cry2^{-/-}$ cells are treated with the anticancer drug, oxaliplatin, the $p53^{-/-}$ tumors continue to grow whereas the $p53^{-/-}Cry1^{-/-}Cry2^{-/-}$ tumors exhibit extensive apoptosis and stop growing. This finding provides a mechanistic foundation for overcoming the resistance of p53-deficient tumor cells to apoptosis induced by DNA-damaging agents and suggests that disruption of cryptochrome function may increase the sensitivity of tumors with p53 mutation to chemotherapy.

TABLE OF CONTENTS

LIST OF TABLES

LIST OF FIGURES

LIST OF ABBREVIATIONS AND SYMBOLS

BMAL	brain and muscle aryl hydrocarbon receptor nuclear translocator (ARNT)-like
cDNA	complementary DNA
C-EBPα	CCAAT-enhancer-binding protein α
ChIP	chromatin immunoprecipitation
Cry	cryptochrome
CyPB	cyclophilin B
DBD	DNA-binding domain
DMEM	Dulbecco's modified Eagle's medium
DTT	dithiothreitol
EDTA	ethylenediaminetetraacetic acid
Egr1	early growth response protein 1
FBS	fetal bovine serum
FDG	fludeoxyglucose
GAPDH	glyceraldehyde 3-phosphate dehydrogenase
GFP	green fluorescent protein
hr	hour
ID	injected dose
Kg	kilogram
MAP	maximum a posteriori probability algorithms
mg	milligram
μg	microgram
min	minute
mL	milliliter

μM	micromolar
NaCl	sodium chloride
NOD	non-obese diabetic
NP40	nonylphenoxypolyethoxylethanol
OD	oligomerization domain
PAGE	polyacrylamide gel electrophoresis
PARP	Poly (ADP-ribose) polymerase
PBS	Phosphate buffered saline
PCR	polymerase chain reaction
Per	period
PET	positron emission tomography
qPCR	quantitative real time polymerase chain reaction
Ras	Rous sarcoma
ROI	region of interest
RT-PCR	reverse transcriptase PCR
SDS	sodium dodecyl sulfate
SCID	severe combined immune deficiency
siRNA	small interfering RNA
TAD	transactivation domain
TTFL	transcription-translation feedback loop
UV	ultraviolet
Z-DEVD-FMK	Z-Asp(OMe)-Glu(OMe)-Val-Asp(OMe)-CH_2F

INTRODUCTION

Circadian Clock

A variety of biological systems in living organisms ensure proper adaptation to constantly changing environmental conditions. The most obvious conditions that affect most living organisms, from bacteria to humans, is the daily (circadian) light-dark cycle caused by the Earth's rotation around its axis. To ensure proper adaptation to the circadian cycle, many organisms have developed a global regulatory system called the circadian clock that generates rhythmic changes with about 24-hr periodicity in many cellular and organismal functions (Bell-Pedersen et al., 2005; Lowrey and Takahashi, 2004). Thus, in mammals, various physiological processes including the daily sleep and wake cycle, blood pressure, body temperature, feeding behavior, hormone secretion, drug and xenobiotic metabolism, glucose homeostasis, cell-cycle progression, and immune system activity demonstrate circadian oscillation even in the absence of environmental cues (Merrow et al., 2005).

Following the initial discovery of circadian clock genes in mammals, it became clear that the expression of these genes was ubiquitous and has the capacity for generating circadian oscillations in various gene expressions in the majority of tissues throughout the body (Bell-Pedersen et al., 2005; Lowrey and Takahashi, 2004). It is now well established that the circadian clock is operative in virtually every cell and tissue and that clock function at the molecular level is determined by interlocking transcription-translation-based feedback loops (TTFL) that drive rhythmic RNA and protein expression of key clock components. At the molecular level the clock is comprised of 4 gene groups, *CLOCK/NPAS2*, *BMAL1*,

Cry1/2, and *Per1/2*, that generate a transcription-translation feedback loop (TTFL) (Fig. 1): The transcriptional activators CLOCK and BMAL1 proteins, which belong to the family of bHLH-PAS domain transcription factors, make a heterodimer that binds to E-box enhancer elements (CACGTG) in the promoter of the transcriptional repressor genes Cryptochrome 1 and 2 (Cry1 and Cry2) and Period 1 and 2 (Per1 and Per2) and induces their transcription. The Cry and Per proteins, in turn, inhibit the CLOCK-BMAL1 after a time lag to close the regulatory loop and generate rhythmic expression or subcellular location of the clock proteins (Hastings et al., 2003; Reppert and Weaver, 2002; Sahar and Sassone-Corsi, 2009; Sancar, 2008; Takahashi et al., 2008; Vitaterna et al., 1999). The time delay between the synthesis of the Per and Cry and their action as repressors is a key factor in generating an oscillatory pattern of expression of these proteins (Lee et al., 2001). The entire cycle takes approximately 24 hours to complete; however, little is known about the stoichiometry and kinetics of this feedback loop. In addition to the primary feedback loop, there is a second negative-feedback loop involving the nuclear hormone receptor Rev-Erbα, which is a direct target of CLOCK-BMAL1 and which strongly represses BMAL1 transcription (Preitner et al., 2002; Sato et al., 2004). This secondary loop is not essential, but is thought to add robustness to the circadian clock (Gallego and Virshup, 2007; Lee et al., 2001).

In addition to the core components of circadian oscillatory machinery, the Clock-BMAL1 complex drives the rhythmic expression of numerous clock controlled genes harboring E-box sequences in their promoters, providing a complex multilevel regulation of the circadian clock which ensures high plasticity of the system and enabling fast adaptation of the organism to its constantly changing environment (Grundschober et al., 2001; Lowrey and Takahashi, 2004; Panda et al., 2002; Storch et al., 2002).

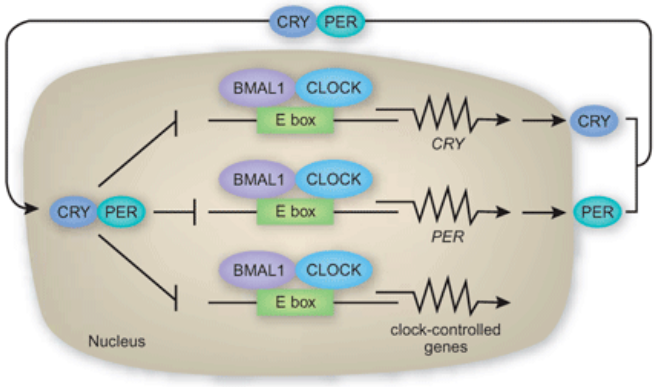

Fig. 1. Mammalian molecular clock. BMAL1-CLOCK heterodimer binds to the E-boxes in the promoters of the *PER* and *CRY* genes, as well as in the clock-controlled genes, activating their transcription. After a time lag, the Per and Cry proteins dimerize, enter the nucleus and inhibit CLOCK-BMAL1-activated transcription of their own genes as well as of those of clock-controlled genes, thus generating an oscillatory pattern of gene expression. Adapted from (Hastings et al., 2003; Reppert and Weaver, 2002; Sahar and Sassone-Corsi, 2009; Sancar, 2008; Takahashi et al., 2008; Vitaterna et al., 1999).

Thus, the circadian clock system regulates physiology, behavior, and metabolism through periodic activation and repression of the set of clock-controlled genes (CCGs) that are involved in a remarkably wide variety of cellular pathways (Green et al., 2008; Sahar and Sassone-Corsi, 2009; Schibler and Sassone-Corsi, 2002). Global temporal transcriptional profiling of various tissues using microarray hybridization approaches has revealed that as much as 10% of mammalian transcriptome oscillate in a circadian manner (Panda et al., 2002). Furthermore, these studies demonstrate remarkable tissue-specificity of circadian regulation with less than 5-10% overlap in clock-controlled genes between different tissues.

In many cases, tissue-specific clock-controlled genes were recognized to be involved in rate-limiting steps that were distinct for the organ function (Panda et al., 2002; Storch et al., 2002). In addition to their primary role in the generation of circadian rhythms, recent work has shown that circadian clock genes can affect a wide variety of other physiological processes. Accordingly, the clock network is integrated within all of the major cellular signaling and metabolic pathways (Hastings et al., 2003; Sahar and Sassone-Corsi, 2009; Takahashi et al., 2008). As a consequence, disruption of the clock is expected to affect cellular and organismal behavior in multiple ways. Emerging examples of circadian regulation of physiological pathways include diverse aspects of cellular metabolism, cell growth and DNA-damage control, xenobiotic responses, and the modulation of behavioral responses to drugs and alcohol. Thus, it has been widely recognized that these periodic rhythms are capable of responding to environmental changes to coordinate the phases of the endogenous clocks with intracellular or extracellular environment.

Cryptochrome

Cryptochrome (Cry) is a flavoprotein that regulates growth and development in plants

in response to blue light, functions as a circadian photoreceptor in *Drosophila* and other insects, and acts as a core component of the molecular clock in mammalian organisms (Cashmore, 2003; Lin and Shalitin, 2003; Partch et al., 2005; Partch and Sancar, 2005; Sancar, 2004a, b). Cryptochrome exhibits 25-50% sequence identity to photolyase (Hsu et al., 1996; Todo et al., 1996) and, like photolyases, contains both FAD and folate as cofactors (Lin et al., 1995; Malhotra et al., 1995). Most cryptochromes, including the human cryptochrome, have C-terminal extensions of 20–200 amino acids beyond the photolyase homology region. Of all cryptochromes identified to date, the *Arabidopsis* cryptochrome is the best characterized. However, despite numerous findings indicative of a photoreceptor function of cryptochrome in *Arabidopsis*, the photochemical reaction in blue-light signaling by cryptochrome is not known and still the strongest evidence that *Arabidopsis* cryptochrome are blue-light receptors is their high degree of similarity to photolyase (Cashmore, 2003; Lin and Shalitin, 2003; Sancar, 2003).

Based on exhaustive biochemical data, it has been concluded that humans and other placental mammals do not have photolyase (Li et al., 1993). Therefore, the discovery of cryptochrome as a photolyase ortholog by the human genome project was rather surprising and necessitated reevaluation of the issue of photolyase in humans. These studies demonstrated that neither this protein nor a second ortholog our group subsequently discovered had photolyase activity and suggested that these proteins must therefore perform other blue light-dependent functions in human cells (Hsu et al., 1996). Taking into account the information available on circadian photoreception at the time, it was proposed that these proteins may function as circadian photoreceptors (Hsu et al., 1996).

To test the hypothesis that cryptochrome functions as circadian photoreceptors, the expression pattern of Cry1 and Cry2 was analyzed. Cryptochrome was found to be expressed in all tissues; however, expression was high in the retina and restricted to the inner retina in both mice and humans (Miyamoto and Sancar, 1998, 1999; Thompson et al., 2003). In the brain of mice, Cry1 was highly expressed in the anterior hypothalamus in a cluster of neurons called the suprachiasmatic nuclei (SCN), and expression exhibited a daily oscillation, peaking at about 2:00 p.m. and reaching its nadir at around 2:00 a.m. (Miyamoto and Sancar, 1998, 1999). Thus, it appeared that cryptochrome was expressed in the appropriate places for setting the clock and for running it and gave credence not only to the hypothesis that cryptochrome is a circadian photoreceptor but also raised the possibility that cryptochrome is a component of the molecular clock (Miyamoto and Sancar, 1998). Subsequently, cryptochrome was found in *Drosophila* and all other insects tested as well as *Xenopus* and all other vertebrate animals whose genomes have been sequenced (Hall, 2000; Sancar, 2000; Todo, 1999).

At present, there is no crystal structure of any animal cryptochrome. Molecular modeling of the human Cry2 photolyase homology region using the structure of *Arabidopsis* Cry1 as a template (Brautigam et al., 2004) reveals a photolyase-like structure including the positively charged DNA-binding groove (Fig. 2) (Brautigam et al., 2004; Ozgur and Sancar, 2003; Sancar, 2004b). Both human Cry1 and Cry2 bind with moderate affinity to DNA and with higher affinity to UV light-damaged DNA but have no repair activity (Ozgur and Sancar, 2003).

The DNA binding activity of cryptochrome might be an evolutionary relic of its common ancestry with photolyase. In contrast to these biochemical activities of obscure

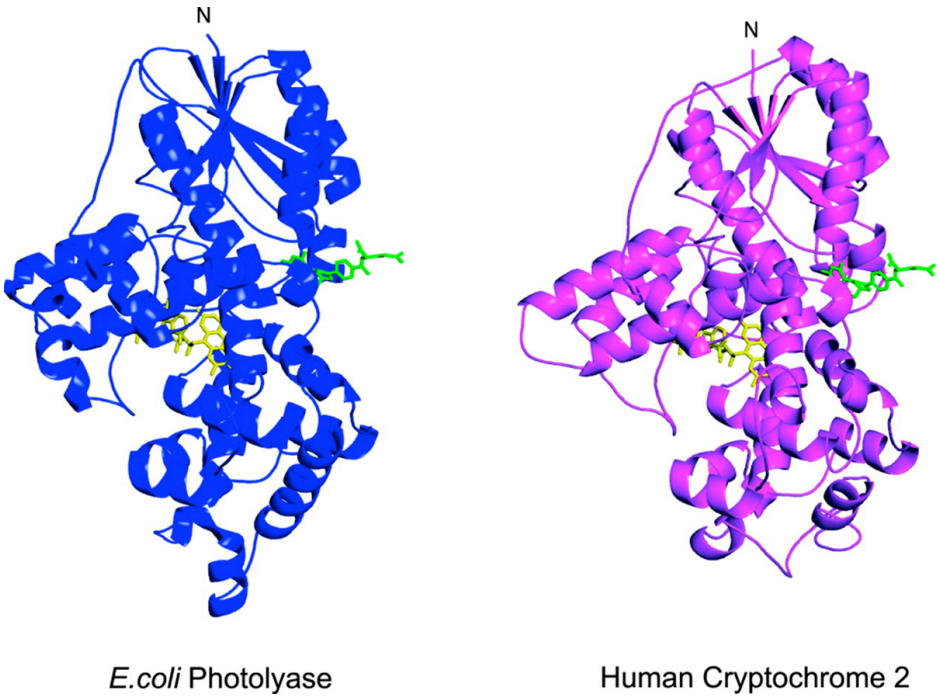

Fig. 2. Structures of photolyase and cryptochrome. *Left*, crystal structure of *E. coli* photolyase; *right*, the computer-generated structure of human cryptochrome 2. *Yellow*, FAD; *green*, MTHF. Adapted from (Ozgur and Sancar, 2003; Sancar, 2004b).

significance, human cryptochrome interacts strongly with several "clock proteins" to generate a transcriptional feedback loop called the circadian clock (Reppert and Weaver, 2002; Young and Kay, 2001). The first direct evidence that cryptochrome plays a role in the circadian clock came from the analysis of mice in which the *Cry2* gene was knocked out: Wild type mice in constant darkness exhibit a circadian rhythm of behavior with an intrinsic period of 23.7 h. The $Cry2^{-/-}$ mice exhibited a period about 1 h longer than wild type mice (Thresher et al., 1998). These data led to the conclusion that Cry2, in addition to any putative photoreceptor function, must have a light-independent role in the maintenance of the normal rhythm (Thresher et al., 1998). This conclusion was strengthened and extended by the analysis of mice lacking Cry1 or both Cry1 and Cry2 (van der Horst et al., 1999; Vitaterna et al., 1999); $Cry1^{-/-}$ mice have a period 1 h shorter than wild type mice and, most strikingly, $Cry1^{-/-}Cry2^{-/-}$ (hereafter Cry^{DKO}) animals are arrhythmic. The cause of the drastic effect of the loss of cryptochrome became apparent when the molecular basis of the mammalian circadian rhythm was elucidated (Fig. 1) (Reppert and Weaver, 2002; Young and Kay, 2001).

p73 Tumor Suppressor

One of the most significant advances in cancer biology in recent years has been the recognition of the importance of apoptosis in preventing oncogenically transformed cells from proliferation and hence from overt cancer (Johnstone et al., 2002). It appears that oncogenically transformed cells are more prone to apoptosis than normal cells (Junttila and Evan, 2009). The tumor suppressor protein p53 is a master regulator of the apoptotic cellular response to DNA damaging agents including many anticancer drugs (Fridman and Lowe, 2003; Lowe et al., 1994; Lowe et al., 1993; Meulmeester and Jochemsen, 2008; Symonds et

al., 1994). However, cancers with intact p53 function are in a minority. Indeed, at least 50% of human cancers lack functional p53 (Vogelstein et al., 2000). Furthermore, lack of p53 activity in tumor cells causes resistance to chemo- and radiotherapies and thereby contributes to the progression of the tumor to a more malignant phenotype (Cohen et al., 2005; Lowe et al., 2004; Munro et al., 2005; Schmitt et al., 2002). Nonetheless, p53-deficient cancer cells still leave intact latent potential to undergo apoptosis, implying the existence of other mechanisms of apoptosis (Hollstein et al., 1999; Roos et al., 2004). Thus, elucidation of this tumor-suppressive mechanism is considered to be important for developing strategies to treat p53 mutant tumors.

Investigation of activating p53-related signaling in the absence of any form of p53, structural and functional homologues of the p53 tumor suppressor, p73 and p63, which are also transcription factors, have been identified (Kaghad et al., 1997; Yang et al., 1998). Although p63 and p73 exhibit limited sequence homology with p53 in the N-terminal transactivation domain (TAD) and the C-terminal oligomerization domain (OD), both share approximately 60% similarity with the central DNA-binding domain (DBD) of p53, including conservation of essential DNA contact residues (Yang et al., 2002). This similarity allows p63 and p73 to regulate p53 target genes and, similar to p53, to induce cell cycle arrest and apoptosis (Danial and Korsmeyer, 2004; Urist and Prives, 2002; Yang et al., 2002). Gene knockout studies have shown that in contrast to p53, p63 and p73 play essential roles in development as homozygous knockout of either gene causes embryonic lethality (Mills et al., 1999; Yang et al., 1999; Yang et al., 2000).

In addition to their roles in development, the p53 family members p63 and p73 have been linked to tumor suppression through pro-apoptotic function (Agami et al., 1999; Flores

et al., 2005; Gong et al., 1999; Irwin and Kaelin, 2001; Jost et al., 1997; Stiewe and Putzer, 2000; Yang et al., 1998; Yuan et al., 1999). It has been reported that in the absence of p53, p73 substitutes p53 functions that trigger apoptosis (Irwin et al., 2003). This finding suggests that p73 is a key player in cellular response to anticancer drugs in tumor cells that lack functional p53. Indeed, inhibition of p73 function by dominant-negative p73 variants or small interfering RNA (siRNA) reduces the cytotoxicity of genotoxic drugs (Irwin et al., 2003; Lin et al., 2004). These studies support a model in which in the absence of p53, the functional status of p73 is an important determinant of cellular sensitivity to anticancer drugs. Recent work has shown that p73 is induced by a wide range of chemotherapeutic drugs, including cisplatin, doxorubicin, taxol, and camptothecin (Agami et al., 1999; Costanzo et al., 2002; Gong et al., 1999; Irwin et al., 2003).

Moreover, efforts directed at functional screening for small molecules that restore p53 transcriptional responses in p53-deficient cells suggest that the p73 can promote apoptosis in p53-deficient cells as an important therapeutic target (Wang et al., 2006). Specifically, small molecules that increase expression of p73 restore proapoptotic effects normally observed downstream of wild-type p53 activation by classic therapeutic agents. In addition, the fact that p73 is rarely genetically and epigenetically altered in cancer means it provides a window of opportunity for treatment by increasing p73 expression in nearly all tumor types (Melino et al., 2002; Melino et al., 2003). Moreover, recent preclinical data show that breast cancer patients with high expression of p73 appear to exhibit increased sensitivity to platinum-based chemotherapy (Leong et al., 2007).

Cryptochrome/Carcinogenesis/Apoptosis

Work in our lab on circadian clock-cancer connection revealed that Cry mutation does not predispose mice to spontaneous or IR-induced cancers (Gauger and Sancar, 2005) and that in p53-null background Cry mutation reduced cancer risk (Ozturk et al., 2009). I wished to understand the mechanism by which Cry mutation reduced cancer risk in p53-null animals.

I found that circadian clock disruption by Cry mutation (Ozturk et al., 2009) or Cry downregulation in a p53-null (Lowe et al., 1994; Lowe et al., 1993) background renders cells more sensitive to genotoxic agents, such as UV, by making them more prone to apoptosis (Fig. 3; Fig. 4) (Ozturk et al., 2009). To gain some insight into the mechanism by which Cry mutation sensitizes cells to apoptosis we considered the p53-independent pathways for intrinsic apoptosis.

Specifically, I focused on contribution of the p73 gene to intrinsic apoptosis. The p73 protein along with p63 and p53 constitute the p53 family (Melino et al., 2003; Stiewe, 2007; Yang et al., 2002). Of these, p53 is the primary tumor suppressor which prevents cancer mainly by promoting apoptosis in response to DNA damage or oncogenic transformation. In the absence of p53, the other two members of the family, in particular p73, a structural and functional homolog of p53 (Melino et al., 2003; Stiewe, 2007; Yang et al., 2002), can substitute for p53 as the pro-apoptotic tumor suppressor (Flores et al., 2005; Gong et al., 1999; Irwin et al., 2000; Irwin et al., 2003; Jost et al., 1997).

Hence, when I discovered that $p53^{-/-}Cry1^{-/-}Cry2^{-/-}$ (hereafter $p53^{KO}Cry^{DKO}$) cells have increased sensitivity to apoptosis compared to $p53^{-/-}$ ($p53^{KO}$) cells (Ozturk et al., 2009), I reasoned that this might have been caused by an elevated level of p73 in $p53^{KO}Cry^{DKO}$, in particular after DNA damaging treatment as it is known p73 is a damage-inducible gene

(Marabese et al., 2003). To test this idea I compared the p73 levels and apoptosis in $p53^{KO}$ and $p53^{KO}Cry^{DKO}$ cells after UV irradiation or oxaliplatin treatment. I found that these genotoxic treatments induce high levels of p73 in cryptochrome mutant cells and significantly enhance apoptosis and clonogenic cell death in $p53^{KO}Cry^{DKO}$ cells relative to $p53^{KO}$ cells. Finally, I demonstrated that the circadian clock regulates p73 activity through C-EBPα and Egr1 in the response to DNA damage. These findings suggest that disruption or inhibition of cryptochrome function may be used as an adjuvant in cancer chemotherapy with platinum-based drugs.

A

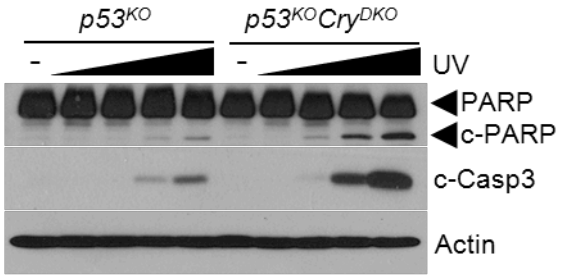
p53KO
p53KOCryDKO
-
-
UV
PARP
c-PARP
c-Casp3
Actin

B

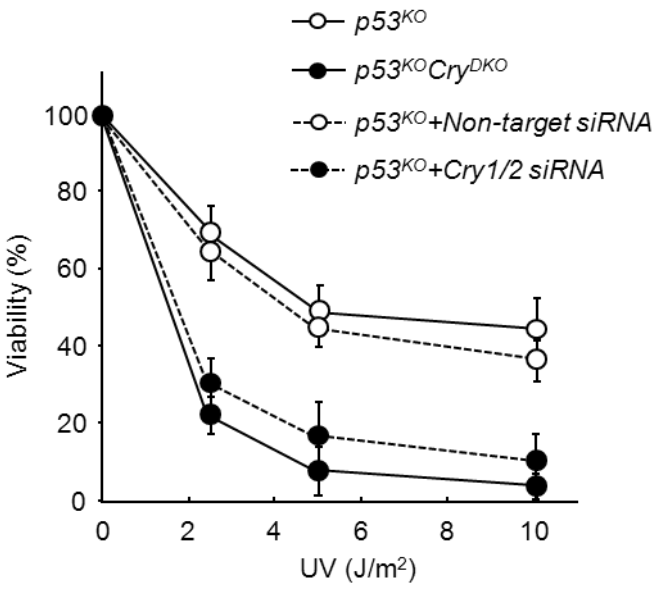
p53KO
p53KOCryDKO
p53KO+Non-target siRNA
p53KO+Cry1/2 siRNA
Viability (%)
100
80
60
40
20
0
0
2
4
6
8
10
UV (J/m2)

Fig. 3. p53-null and Cry-deficient cells are more sensitive to UV-induced apoptosis and clonogenic death than *p53*^{KO} cells. (*A*) Apoptosis. Unirradiated (-) or irradiated (2,5,10,20 Jm^{-2}) cells of the indicated genotypes were harvested 24 hrs post-irradiation, lysed and analyzed by immunoblotting. (*B*) Clonogenic survival. Cells of the indicated genotypes, transfected with indicated siRNAs for 48 hrs, were irradiated with the indicated UV dose and then incubated for 9-10 days until colonies were readily visible. Results represent the means of 3 independent experiments (±s.d.). From (Ozturk et al., 2009)

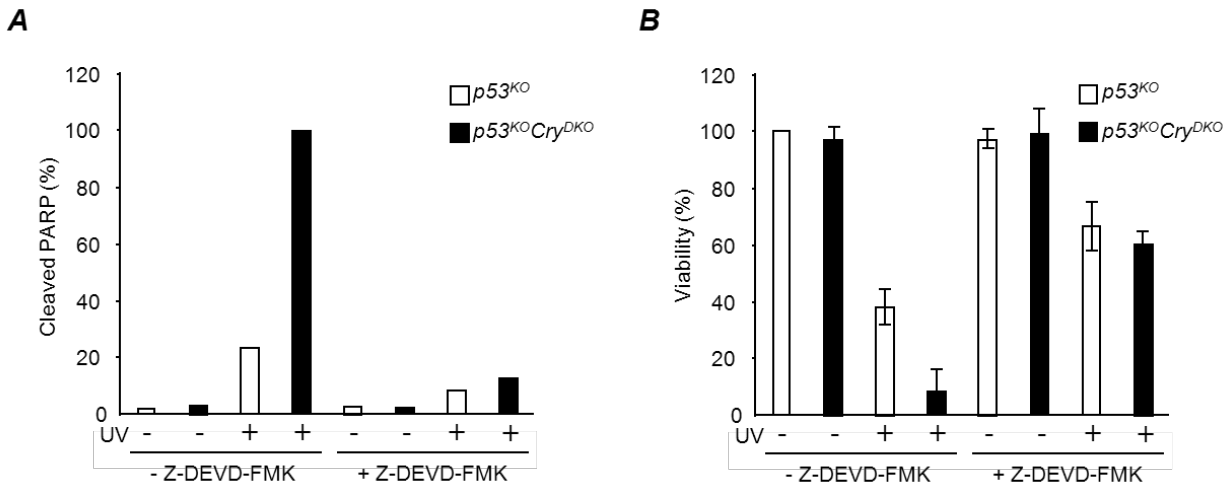

Fig. 4. Increased UV-killing of p53-null and Cry-null cells is due to enhanced apoptosis. Cells of the indicated genotypes were preincubated for 2 hrs with the caspase 3 inhibitor, Z-DEVD-FMK, where indicated, irradiated with 10 Jm^{-2} and analyzed for apoptosis and UV survival. (*A*) Apoptosis. The maximum value of cleaved PARP was set to 100% and other values are plotted relative to the maximum. (*B*) UV survival. Standard clonogenic assay was used to obtain percent survival. Means (±s.d.) of 3 independent experiments.

MATERIALS AND METHODS

Establishment of $p53^{KO}$ and $p53^{KO}Cry^{DKO}$ Tumor Cell Lines

The cell lines were generated from the $p53^{KO}$ and $p53^{KO}Cry^{DKO}$ mouse strains as described previously (Gauger and Sancar, 2005; Ozturk et al., 2009). To obtain cell lines, skin patches from the back of mice at the age of 3 months were taken under sterile conditions, cut into small pieces, placed into 4 or 6 well-plates and incubated for one week to let the fibroblasts migrate into the wells. The fibroblasts were passaged at least 3 times before using them in any experiments. Primary wild-type skin fibroblasts were isolated in the same manner, and passaged 8 times without the appearance of spontaneously immortalized clones. Wild-type mouse embryonic fibroblasts were kindly provided by Dr. Norman Sharpless (University of North Carolina). For *Ras*-induced oncogenic transformation, cells were seeded into 10 cm plates, and transfected with 250 ng of pEGFP-N1 (Clontech), and/or 5 μg of *Ras* pT24 vector (Ozturk et al., 2009) using FuGENE 6 reagent (Roche). The next day, cells were split into 3 plates, and incubated for 18 days. The plates were stained with Giemsa and colonies of oncogenically transformed cells were counted visually and the fraction of transformed cells was normalized for transfection efficiencies calculated by counting GFP positive cells in each plate. These cells were maintained in DMEM (Life Technologies, Gaithersburg, MD) supplemented with 10% fetal bovine serum (Gemini, Woodland, CA) and 100 units/mL penicillin and 100 μg/mL streptomycin (Life Technologies). The cells were maintained in an incubator at 37°C under 5% CO_2. The Cry^{DKO} cell line has been described (Gauger and Sancar, 2005).

Human Cell Lines

The H1299 cells were kindly provided by Dr. Shlomo Melmed (Cedars-Sinai Medical

Center, LA). Caco-2 and A549 cells were obtained from American Type Culture Collection (ATCC). These cells were grown in DMEM with 10% FBS and 100 units/mL penicillin and 100 μg/mL streptomycin at 37°C under 5% CO_2.

Clonogenic Survival Assay

UV survival assays were performed as described previously (Gauger and Sancar, 2005) using a fluence in the range of 0-10 Jm^{-2}. For oxaliplatin survival assays, cells were seeded into 6-well plates at 10^5, 5×10^4, and 2×10^4 cells per well in duplicate and incubated in growth medium for 10 to 14 hrs. The cells were washed and incubated with 0-20 μM oxaliplatin for 2 hrs. Then, the cells were washed with PBS twice, growth medium was added and cells were incubated for 10 to 14 days. Cells were then fixed for 20 min in 3:1 methanol/acetic acid, rinsed with water, and stained with 5% methylene blue, and counted. Colonies containing >50 cells were scored and survival was calculated from the ratio of the number of colonies in the treated samples to those in the control plates.

Immunoblot Analysis

Antibodies were from the following sources: Egr1, PARP, cleaved Caspase 3, p53 (Cell Signaling Technology), p63 (Novus Biologicals), p73 (Upstate), C-EBPα (Thermo Scientific), and Actin, Cyclophilin B (Santa Cruz Biotechnology). Mouse Cry1 (monoclonal) and Cry2 (polyclonol) antibodies were made in our laboratory (Gauger and Sancar, 2005). Conventional immunoblotting procedures were used to detect the target proteins: Cells were collected, washed once in cold PBS and then scraped in TEGN buffer (10 mM Tris at pH 8, 1 mM EDTA, 10% glycerol, 0.5% NP40, 400 mM NaCl, 1 mM DTT, 0.5 mM phenylmethylsulfonylfluoride, and protease inhibitor mixture containing 1 M Benzamidine, 3

mg/mL Leupeptin, 100 mg/mL Bacitracin, and 1 mg/mL α_2 macroglobulin) and incubated on ice for 15 min. Lysates were then cleared by centrifugation at 20,000 g for 10 min. Total protein concentration was determined via the Bio-Rad protein assay (Bio-Rad Laboratories). Equal amounts of protein were separated on 10% SDS-PAGE and the proteins were transferred to nitrocellulose membranes (Schleicher and Schuell). The membranes were then blocked for 1 hr in a PBS solution containing 5% nonfat milk powder and 0.1% Tween-20 and then probed with primary antibody overnight in 1% milk, 0.1% Tween-20 in PBS. After washing, membranes were incubated for 1 hr with horseradish peroxidase-linked secondary antibody (Sigma) in 1% milk, 0.1% Tween-20 in PBS. Finally, after three 5-min washes in 0.1% PBS-Tween 20, proteins were visualized by enhanced chemiluminesence (Amersham Biosciences). Band intensities were quantified with ImageQuant 5.2 software (Molecular Dynamics).

Chromatin Immunoprecipitation

ChIP was performed by manufacturer's instruction (Sigma) with some exceptions. Protein-DNA complexes incubated with rabbit polyclonal antibodies against BMAL1 (Bethyl Laboratories, Inc.), rabbit monoclonal antibody directed against Egr1 (44D5, Cell Signaling Technology), rabbit polyclonal antibody against C-EBPα (PA1-825, Thermo Scientific), or equivalent IgG control (Cell Signaling Technology) were precipitated using protein A/G-conjugated agarose beads (Calbiochem). Protein-DNA crosslink was resolved and followed by quantitative real-time PCR (qPCR) using sybr green master mix (Applied Biosystems) with the primers listed in Table 1.

Chemicals and Treatment

Cells were treated with 20 μg/ml cycloheximide (Sigma) or 5 μg/ml actinomycin D in DMEM as indicated and then protein stability was assayed by conventional immunoblotting. The caspase 3 inhibitor Z-Asp(OMe)-Glu(OMe)-Val-Asp(OMe)-CH_2F (Z-DEVD-FMK) (R&D systems, Inc.) was used at a final concentration of 25 μM.

RNA Interference and Transfection

For RNAi experiments, cells at 70% confluency were transfected using DharmaFECT (Dharmacon Research Inc.) according to the manufacturer's directions for transfection of ON-TARGET plus SMARTpool small interfering RNA (siRNA) duplexes specific for each target purchased from Dharmacon Research Inc; mouse Cry1 (L-040485-01-0005), mouse Cry2 (L-040486-00-0005), mouse Per1 (L-040487-00-0005), mouse Per2 (L-040489-01-0005), mouse BMAL1 (L-040483-01-0005), mouse Egr1 (L-040286-00-0005), mouse C-EBPα (L-040561-00-0005), mouse p73(L-043871-00-0005), mouse cyclophilin-B (D-001820-20-05) as a control, human Cry1 (L-015421-00-0005), human Cry2 (L-014151-01-0005), human cyclophilin-B (D-001820-10-05) as a control, or non-targeting siRNA (D-001810-10-05) as a control. The siRNA experiment was carried out for 48 hrs, at which time cells were harvested and the extent of knockdown of the target genes was assessed by immunoblotting or RT-PCR. For the determination of the effect of gene knockdown on clonogenic survival, after treating the cells with siRNA for 24 hrs, the cells were plated at low density to ensure the formation of 400 colonies per 6-well plate in the absence of UV irradiation. Following plating, cells were incubated in growth medium for 10 to 14 hrs and treated with UV at a fluence rate of 0.5 $Jm^{-2}sec^{-1}$ from a germicidal lamp for the appropriate doses. The cells were then incubated for 9 to 10 days until colonies were readily visible. The specificity of the antibodies and siRNAs used are shown in Fig. 5.

RT-PCR

RNA was extracted from cell pellets using RNeasy Mini Kit (Qiagen) and quantified by UV-Vis spectrophotometry. The cDNAs were generated by reverse transcription with random hexamer using ImProm-II Reverse Transcription System (Promega). Then RT-PCR was performed with the primers listed in Table 2. qPCR was then performed using the Expand High Fidelity PCR system (Roche). Conditions for linear amplification were established through template and cycle curves. PCR products (40% of reaction mixture) were then separated on 2% agarose gels and bands were visualized with ethidium bromide staining. Quantification of p73 induction was performed with Image Quant 5.2 software (Molecular Dynamics).

Tumor Xenograft Model

Animal studies were conducted in accordance with the regulations of the National Institutes of Health and the Institutional Animal Care and Use Committee of the University of North Carolina School of Medicine. Tumor xenografts were established in 6-week-old female immunodeficient NOD/SCID mice by subcutaneous inoculation of 2×10^6 cells mixed with an equal volume of matrigel (BD Biosciences) into both flanks. The NOD/SCID mice were bred and kept under defined-flora pathogen-free conditions at the AALAC-approved Animal Facility of the Division of Experimental Radiation Oncology, University of North Carolina. Oxaliplatin at 10 mg/kg was administered intraperitoneally once a week for 21 days. Tumor volume and body weight were recorded every 3 days. Tumor size was measured with a caliper in 3 mutually perpendicular diameters (a, b, and c) and the volume was calculated as $V = (\pi/6)\times a\times b\times c$.

MicroPET Imaging

Whole-body images of the biodistribution of ^{18}F-2-deoxyglucose ([^{18}F]-FDG) tracers in mice was obtained by micro positron emission tomography (microPET) scans. Mice were kept warm, under gas anesthesia (2% isoflourane) and injected with [^{18}F]-FDG intraperitoneally. A 1-h interval for uptake was allowed between probe administration and microPET scanning. Data were acquired using a Siemens Preclinical Solutions microPET Focus 220 instrument. MicroPET data were acquired for 10 min and was reconstructed using statistical maximum a posteriori probability algorithms (MAP) into multiple frames. The spatial resolution of microPET is approximately 1.5-mm, 0.4-mm voxel size. Three-dimensional regions of interest (ROI) were drawn using AMIDE software (Andreas Loening). Color scale is proportional to tissue concentration with red being the highest and lower values in yellow, green, and blue.

In Vivo Imaging of Caspase 3 Activity

For preparation of Z-DEVD-aminoluciferin, 10 mg of Vivo Glo Caspase 3/7 substrate (Promega) were dissolved in 67 µl of surfactant mix (70 µl of Tween 80, 640 µl of PEG 400, and 290 µl of *N,N*-dimethylacetamide) and then added to 100 µl of 5% glucose in water. The mixture was vortexed to make a homogenous suspension and injected intraperitoneally into tumor-bearing mice (100 µl/mouse). 10 minutes after Z-DEVD-aminoluciferin injection, the mice were imaged with IVIS-200 (Xenogen Corp) for the *in vivo* photon counting of bioluminescence. The photon emission intensity (photons/second) of each mouse is indicated in a rainbow bar scale.

Statistical Analysis

Results are shown as mean ± SD, which were performed using 2-tailed *t* test.

Table 1. Primer sequences for ChIP

Gene		Sequence to 5' to 3'	Protein
Egr1	F	CTCCCTCACTGCGTCTAAGG	BMAL1
	R	CACCCAGAATCGAAAGGCTA	
p73	F	GGACTTTGAAGAGTCCAACC	Egr1
	R	CGCTGCCCTTACTGTCCTAA	
p73	F	CCACTGCCTTTGGAGCTAAG	C-EBPα
	R	GCGAGCTGCAGATTAGAGAC	

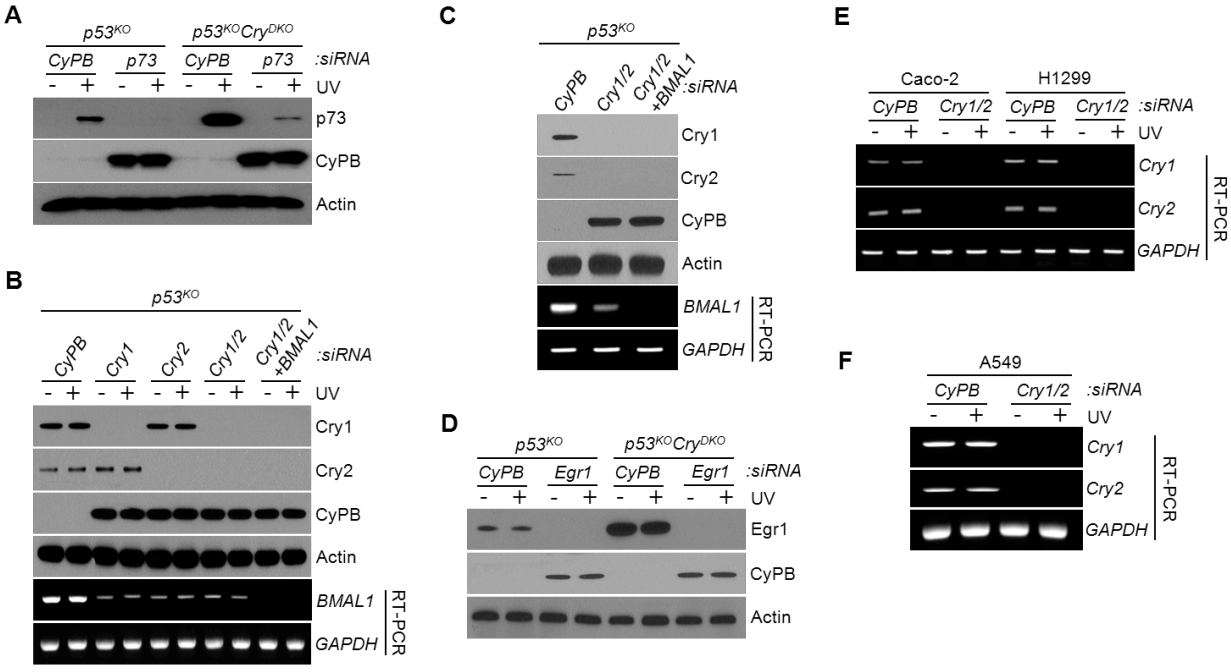

Fig. 5. Specificity and efficiency of siRNAs used to downregulate apoptosis and clock genes. (*A* to *D*) Mouse cell lines. (*E* and *F*) Human cell lines. When available, antibodies were used to monitor downregulation; otherwise RT-PCR was employed for the mRNAs of target genes.

Table 2. Primer sequences

Name		Sequence to 5' to 3'	Species
p73	F	ACCTTCGACACCATGTCTCC	Mouse
	R	GCGAGGTTGTTGCCTTCTAC	
BMAL1	F	CGAAGACAATGAGCCAGACA	Mouse
	R	AAATAGCTGTCGCCCTCTGA	
Per1	F	CTGGCTCCTCCAGTGATAGC	Mouse
	R	CGCTTGGTTGTACTGGGAAT	
Per2	F	AGGATGTGGCAGGTAACAGG	Mouse
	R	TGTACAGTGTGGGGGTGCTA	
GAPDH	F	GGTGAAGGTCGGTGTGAACG	Mouse
	R	CTCGCTCCTGGAAGATGGTG	
Cry1	F	GGCGTTATTTGCCTGTCCTA	Human
	R	ACGTTTCCCACCACTGAGAC	
Cry2	F	GTCCTGCAGTGCTTTCTTCC	Human
	R	CCACACAGGAAGGGACAGAT	
GAPDH	F	ACAGTCAGCCGCATCTTCTT	Human
	R	TTGATTTTGGAGGGATCTCG	

RESULTS

Effect of Cryptochrome Mutation on p73 Expression

I found that under our assay conditions neither p73 nor p63 are detectable before DNA damage but both are strongly induced after UV irradiation (Fig. 6*A*). Importantly, however, while the Cry mutation in p53-null background had no effect on p63 induction by UV it enhanced the rates of both p73 mRNA and protein synthesis by a factor of about 10 (Fig. 6*B*). I should note, however, that the enhanced induction of p73 by UV in $p53^{KO}Cry^{DKO}$ cells is not unique to cells with p53-null genotype. I found essentially the same dose response and enhanced induction of p73 in Cry^{DKO} cells as in $p53^{KO}Cry^{DKO}$ cells (Fig. 7), indicating that enhanced expression of p73 in Cry-null cells is independent of the p53 status of the cell.

To ascertain that the enhanced apoptosis in $p53^{KO}Cry^{DKO}$ was in fact dependent upon p73, I compared the UV-induced apoptosis in $p53^{KO}Cry^{DKO}$ and $p53^{KO}$ cells before and after siRNA knockdown of p73. The results indicate that both the residual apoptosis observed in $p53^{KO}$ and the enhanced apoptosis seen in $p53^{KO}Cry^{DKO}$ cells are drastically reduced when p73 is downregulated (Fig. 8), suggesting that the enhanced induction of p73 in $p53^{KO}Cry^{DKO}$ is responsible for the increased apoptosis seen in these cells.

Regulation of p73 by the Circadian Clock

These findings suggest a unique regulatory mechanism that is both circadian clock- and DNA damage-dependent. To test this model I analyzed p73 levels and apoptotic response to DNA damage in $p53^{KO}$ cells after downregulation of the negative (Cry1/2 or Per1/2) and positive (BMAL1) elements of the core circadian TTFL.

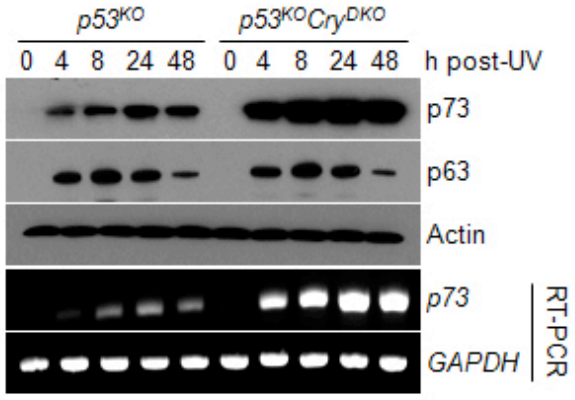
p53KO
p53KOCryDKO
0 4 8 24 48 0 4 8 24 48 h post-UV
p73
p63
Actin
p73
GAPDH
RT-PCR

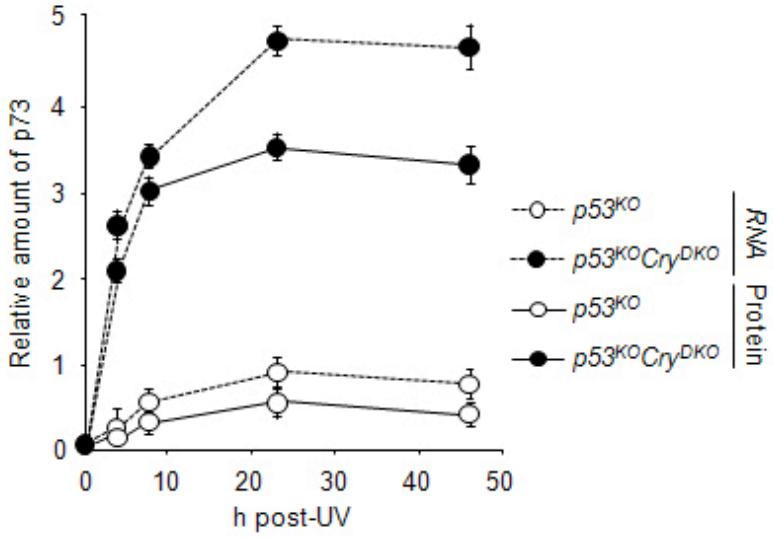
Relative amount of p73
0
1
2
3
4
5
0 10 20 30 40 50
h post-UV
p53KO
p53KOCryDKO
p53KO
p53KOCryDKO
RNA
Protein

Fig. 6. p73 induction is amplified in *p53^{KO}Cry^{DKO}* cells. Time course of p73 induction in *p53^{KO}* and *p53^{KO}Cry^{DKO}* cells analyzed by immunoblotting and RT-PCR. The quantitative results of the levels of p73 protein and mRNA, shown in the bottom panel, are means ±s.d. (n=3). The UV dose was 10 Jm^{-2}.

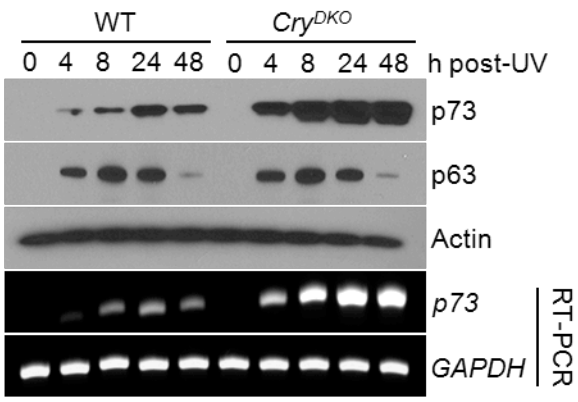

Fig. 7. p73 is highly induced in Cry-null cells by UV irradiation. Cells of the indicated genotypes were irradiated with 10 Jm^{-2} and harvested at the indicated time points. p73 induction was probed by immunoblotting or RT-PCR, using Actin and *GAPDH* as loading controls.

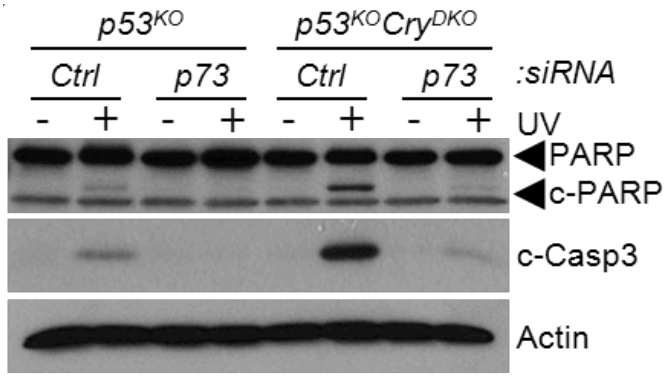

Fig. 8. Enhanced apoptosis in *p53^{KO}Cry^{DKO}* cells is dependent upon p73. Immunoblots showing the role of p73 in UV-induced apoptosis in *p53^{KO}Cry^{DKO}* cells. Cells were transfected with the indicated siRNAs, irradiated with 10 Jm^{-2} and then analyzed for apoptosis by probing for cleaved PARP (c-PARP) and cleaved caspase 3 (c-Casp3).

The results are shown in Fig. 9, and Fig. 10. Downregulation of either Cry1/2 or Per1/2 enhances UV-induced p73 synthesis and apoptosis.

Interestingly, downregulation of either Cry1 or Cry2 yield results similar to downregulation of both genes with regard to UV-induced p73 levels and the extent of apoptosis as probed by caspase activity (Fig. 9). Importantly, both of these effects are reversed by downregulation of BMAL1 (Fig. 9), supporting the conclusion that the expression of p73 is controlled both by DNA damage and by the circadian clock, a unique and unprecedented regulatory mechanism.

Control of p73 Expression by DNA Damage and the Circadian Clock

Next, I wished to find out how clock disruption by Cry mutation leads to elevated p73 levels. As this increase was dependent both on the circadian TTFL and DNA damage we investigated the *p73* promoter for clock-related sequence elements. I found that the *p73* promoter region up to 4 kbp preceding the transcription initiation site did not reveal a canonical E-box or the variant E'-box elements which are key sequence elements in the promoters of most first-order clock-controlled genes. Then, I considered the possibility that p73 may be a second-order clock-controlled gene. The transcriptional regulation of p73 has been investigated in some detail. The gene is negatively controlled by C-EBPα and is activated by Egr1 (Early growth response1) (Marabese et al., 2003; Yu et al., 2007). Treatment of cells with DNA damaging agents leads to release of the repressive C-EBPα from the promoter and transcriptional upregulation of p73 in an Egr1-dependent manner. Of particular interest, it was recently reported that *Egr1* might be a clock-controlled gene (Bai et al., 2008; Humphries and Carter, 2004).

These facts, considered together, lead to certain predictions: Egr1 must be regulated

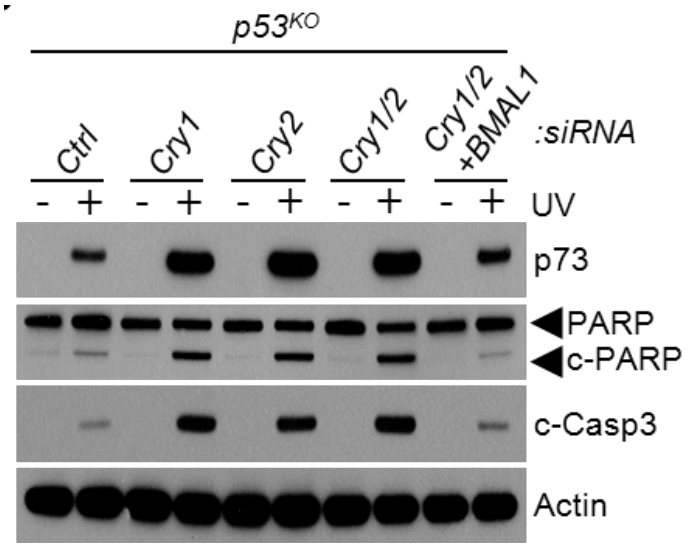

Fig. 9. Regulation of p73-mediated apoptosis by the circadian clock. Enhanced apoptosis observed in cryptochrome-deficient cells is reversed by downregulation of BMAL1. The *p53*^{KO} cells were transfected with the indicated siRNAs, UV irradiated where indicated with 10 Jm^{-2} and apoptosis was probed by immunoblotting for cleaved PARP and cleaved caspase 3.

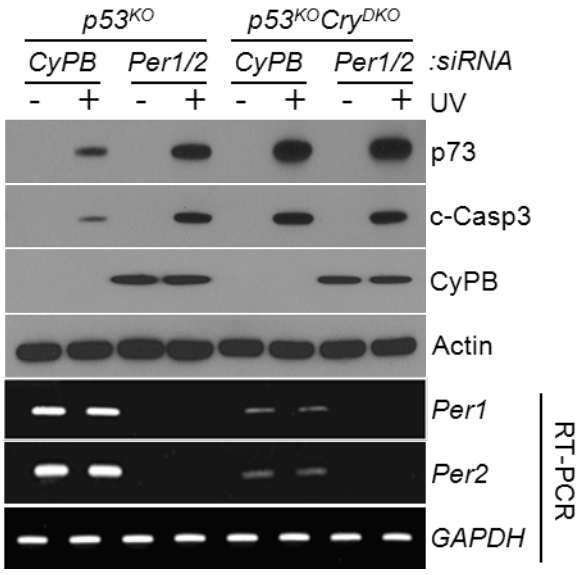

Fig. 10. Downregulation of Period proteins (Per1 and 2) increases sensitivity of *p53^{KO}* cells to UV-induced apoptosis. Cells transfected with the indicated siRNAs were irradiated with 10 Jm^{-2} where indicated and 24 hrs later were harvested and analyzed by immunoblotting for protein expression and apoptosis, and by RT-PCR for gene expression. Actin and *GAPDH* are internal controls for the immunoblots and the RT-PCR reactions, respectively.

in Cry^{DKO} cells and this upregulation must be reversed by downregulation of BMAL1. Secondly, it would be expected that BMAL1 will bind to the *Egr1* promoter, and finally, both Egr1 and C-EBPα are expected to bind to the *p73* promoter where the binding of C-EBPα but not of Egr1 must be affected by UV irradiation.

I tested these predictions in experiments summarized in Fig. 11 and 12. As would be predicted for a clock-controlled gene, the level of Egr1 is elevated both in Cry^{DKO} and $p53^{KO}Cry^{DKO}$ cells (Fig. 11*A*). Moreover, in accordance with the prediction, the elevation of Egr1 as a consequence of Cry downregulation can be reversed by BMAL1 knockdown (Fig. 11*B*), consistent with regulation of Egr1 by the primary circadian feedback loop. In support of the model for positive regulation by BMAL1 and negative regulation by Cry, ChIP analysis reveals occupancy of the *Egr1* E-box sequence element by BMAL1 which is enhanced in the absence of Cry1/2 and abolished by downregulation with BMLA1 (Fig. 11*C*). Finally, when the occupancy of the *p73* promoter was analyzed by ChIP I found greatly enhanced occupancy by Egr1 in $p53^{KO}Cry^{DKO}$ cells, which was not affected by UV irradiation. (Fig. 12*A*). In contrast, Cry mutation had no effect on binding of C-EBPα to the *p73* promoter but the occupancy of the promoter by C-EBPα was drastically reduced after UV irradiation (Fig. 12*A*). Taken together, these data support the model that p73 expression is regulated by the clock-controlled Egr1 and by the DNA damage-controlled C-EBPα and hence in Cry-null mutants increased expression of Egr1 combined with UV damage-induced dissociation of C-EBPα from the *p73* promoter leads to a high level of p73 production and the consequent apoptosis. In further support of this model I found that both in $p53^{KO}$ and in $p53^{KO}Cry^{DKO}$ cells downregulation of Egr1 by siRNA significantly reduces UV induction of p73 and abolishes apoptosis (Fig. 12*B*).

Regulation of p73 by the Circadian Clock in Human Cancer Cell Lines

The apoptosis enhancing effect of Cry mutation seems to be unique to both mouse and human p53 mutant cells because in cells with wild-type p53 the p53-driven apoptosis is expected to be dominant and thus obscure any contribution of the p73 pathway (Flores et al., 2002).

This prediction was tested by analyzing apoptosis in two p53 mutant and one p53 wild-type human cancer cell lines. As seen in Fig. 12*C* in the Caco-2 and H1299 cell lines in which p53 is not functional, downregulation of Cry enhances p73 expression and increases apoptosis after UV irradiation. In contrast, in the A549 cell line with a functional p53 even though downregulation of Cry leads to enhanced levels of p73 after UV this upregulation of p73 is not accompanied by enhanced apoptosis (Fig. 12*D*) because apparently the UV-induced p53 is sufficient to cause maximal level of apoptosis which cannot be further enhanced by increased p73. Taken together, the data in Fig. 11 and 12 show that Egr1 is a clock-controlled gene and that p73 is a second order clock-controlled gene that plays a prominent role in promoting apoptosis in p53-null cells lacking cryptochrome.

Enhancement of the Efficacy of Oxaliplatin by Cryptochrome Disruption

Next, I wished to determine if the enhancement of apoptosis induced by genotoxic agents (intrinsic apoptosis) (Danial and Korsmeyer, 2004; Hotchkiss et al., 2009) by Cry mutation in p53 mutant cells can be used for therapeutic purposes.

Cisplatin and its second and third generation derivatives are UV-mimetic agents that kill cells mainly by producing intrastrand diadducts in DNA (Jung and Lippard, 2007; Kelland, 2007). Hence, I reasoned that cryptochrome disruption might enhance the sensitivity of p53-null cells and tumors to killing by platinum derivatives.

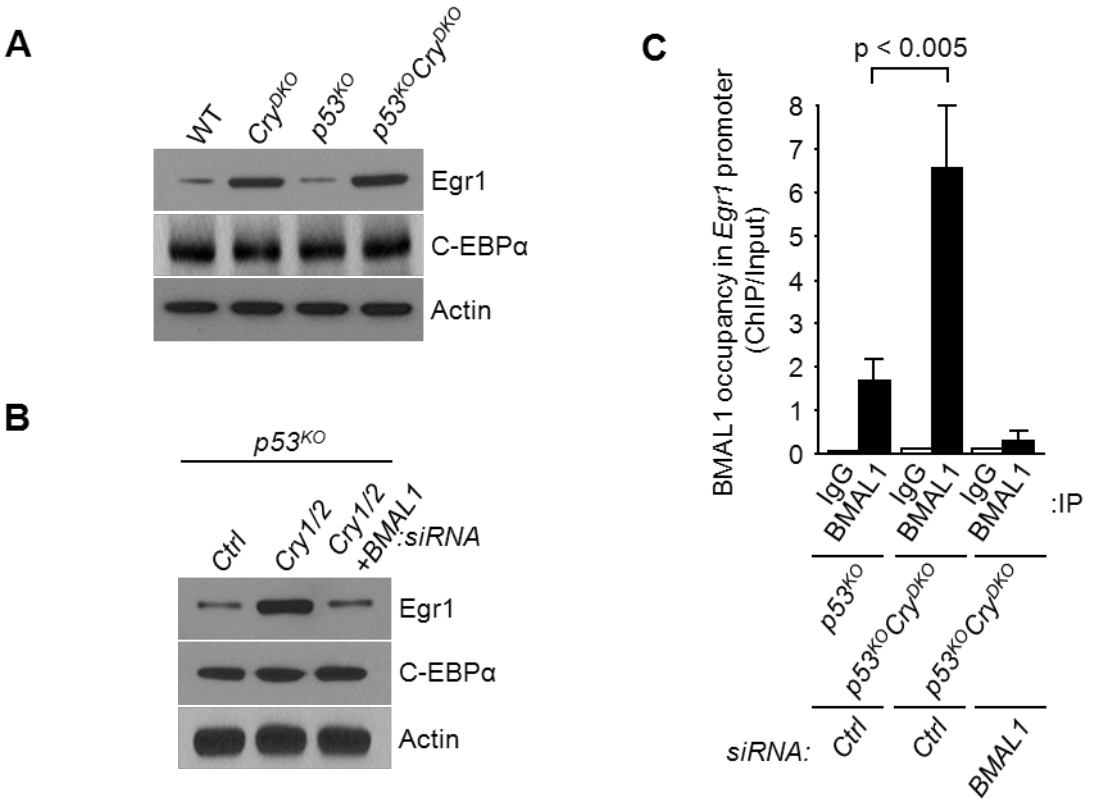
A
WT
Cry^DKO
p53^KO
p53^KO Cry^DKO
Egr1
C-EBPα
Actin
B
p53^KO
Ctrl
Cry1/2
Cry1/2 +BMAL1
:siRNA
Egr1
C-EBPα
Actin
C
p < 0.005
BMAL1 occupancy in Egr1 promoter (ChIP/Input)
0
1
2
3
4
5
6
7
8
IgG
BMAL1
:IP
p53^KO
p53^KO Cry^DKO
siRNA:
Ctrl
BMAL1

Fig. 11. *Egr1* is a clock-controlled gene. (*A*) Overexpression of Egr1 in cryptochrome-deficient cells. Mouse fibroblasts of the indicated genotypes were analyzed for expression of Egr1 and C-EBPα, the two main regulators of p73. Actin was used as a loading control. (*B*) Egr1 expression is regulated by the circadian clock. $p53^{KO}$ fibroblasts were transfected with the indicated siRNAs and the levels of Egr1 and C-EBPα were probed by immunoblotting. (*C*) Binding of BMAL1 (positive arm of the core circadian clock) to the *Egr1* promoter. Fibroblasts of the indicated genotypes were transfected with control (Ctrl) or BMAL1 siRNA and then the occupancy of the *Egr1* promoter by BMAL1 was analyzed by ChIP. Note the elevated ChIP values in $p53^{KO}Cry^{DKO}$ cells relative to $p53^{KO}$ cells, indicating that Cry reduces the occupancy of target promoters by BMAL1 ($p<0.05$, n=3).

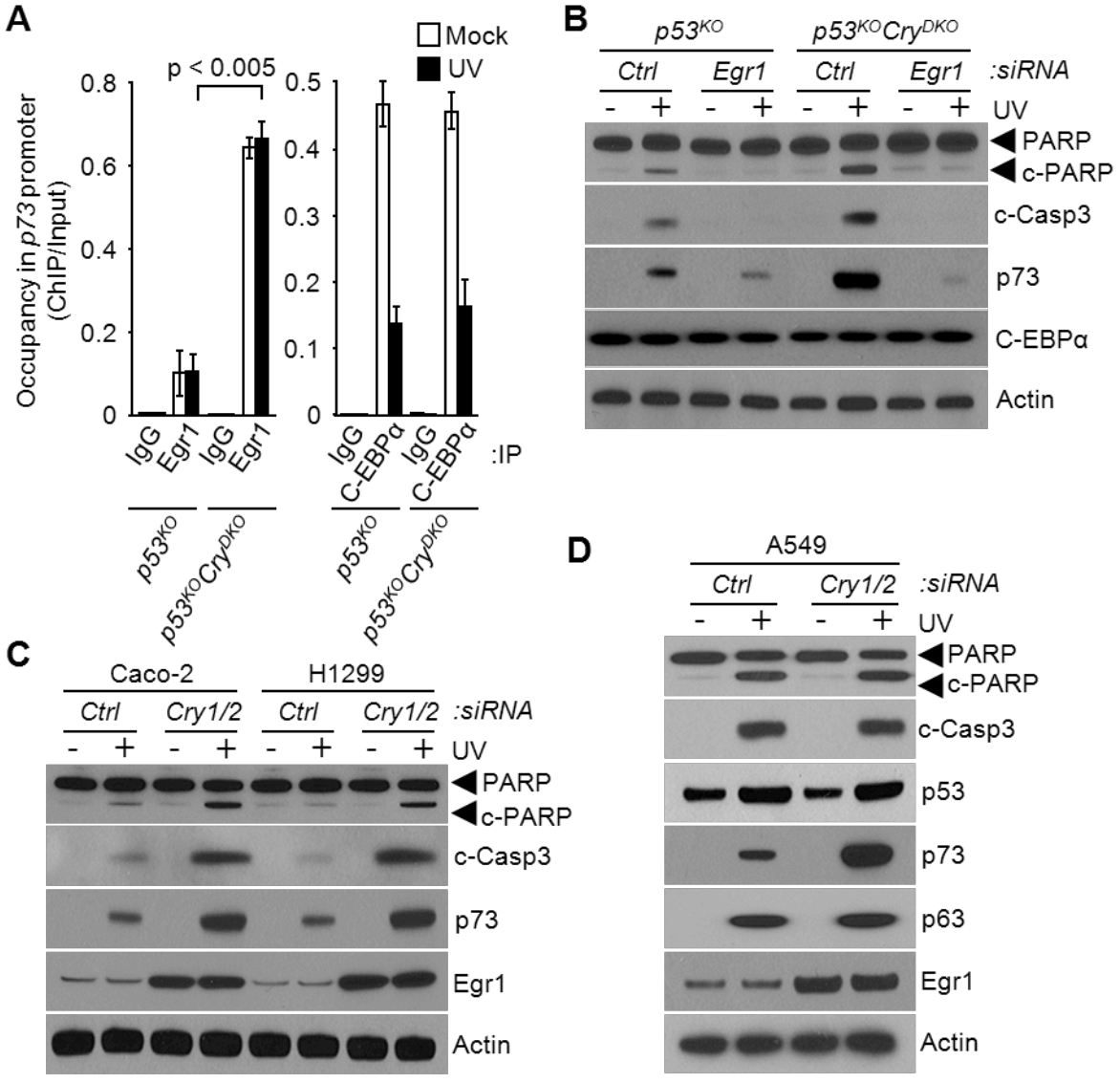
A
Mock
UV
p < 0.005
Occupancy in p73 promoter (ChIP/Input)
0.8
0.6
0.4
0.2
0
0.5
0.4
0.3
0.2
0.1
0
IgG
Egr1
IgG
Egr1
IgG
C-EBPα
IgG
C-EBPα
:IP
p53KO
p53KOCryDKO
p53KO
p53KOCryDKO
B
p53KO
p53KOCryDKO
Ctrl
Egr1
Ctrl
Egr1
:siRNA
- + - + - + - +
UV
PARP
c-PARP
c-Casp3
p73
C-EBPα
Actin
C
Caco-2
H1299
Ctrl
Cry1/2
Ctrl
Cry1/2
:siRNA
- + - + - + - +
UV
PARP
c-PARP
c-Casp3
p73
Egr1
Actin
D
A549
Ctrl
Cry1/2
:siRNA
- + - +
UV
PARP
c-PARP
c-Casp3
p53
p73
p63
Egr1
Actin

Fig. 12. Requirement for Egr1 in the clock-mediated p73-dependent apoptosis. (*A*) Effect of UV on occupancy of *p73* promoter by Egr1 and C-EBPα in the absence and presence of cryptochrome. Mouse fibroblasts of the indicated genotypes were irradiated with 10 Jm^{-2} where indicated and the promoter binding of Egr1 and C-EBPα were determined by ChIP. Note that Cry mutation enhances Egr1 binding ($p<0.05$, $n=3$) which is not affected by UV. In contrast, Cry mutation has no effect on C-EBPα binding, which is significantly reduced by UV irradiation. (*B*) Elevated Egr1 in Cry mutant cells is responsible for enhanced UV-induced apoptosis. Mouse fibroblasts of the indicated genotypes were transfected with the indicated siRNAs, irradiated with UV and then analyzed for C-EBPα and p73 expression directly by immunoblotting, and for apoptosis by immunoblotting for cleaved PARP and caspase 3. (*C*) Effect of cryptochrome downregulation in p53-null human cell lines on Egr1 and p73 expression and UV-induced apoptosis. The cell lines were transfected with the indicated siRNAs, irradiated with 10 Jm^{-2} of UV where indicated and probed for apoptosis by immunoblotting. (*D*) Effect of cryptochrome downregulation on Egr1 and p73 expression and UV-induced apoptosis in a human tumor cell line with wild-type p53. Whole cell lysates were analyzed by immunoblotting.

I performed our chemotherapy experiments with oxaliplatin which is the drug of choice for treating colorectal cancers among others (Kelland, 2007). First, I established that Cry mutation sensitizes transformed p53-null cells to oxaliplatin-induced p73 upregulation and to killing by apoptosis (Fig. 13).

This was to be expected because the major DNA lesions induced by this drug, the GG, AG, and GXG diadducts can only be repaired by nucleotide excision repair as are the cyclobutane pyrimidine dimer and the (6-4) photoproduct (Gauger and Sancar, 2005). Then, I used a mouse tumor model to test the efficacy of oxaliplatin in treating clock-normal and clock-disrupted cancers by oxaliplatin.

Tumor xenografts were established in 6-week-old female immunodeficient mice by injection of oncogenically transformed $p53^{KO}$ and $p53^{KO}Cry^{DKO}$ cells (Ozturk et al., 2009). Each animal received, by subcutaneous injection, $p53^{KO}$ cells in one flank and $p53^{KO}Cry^{DKO}$ cells in the other. The tumors of both genotypes grew at the same rate (Fig. 14), and when the tumor volumes reached 0.1 cm^3 oxaliplatin treatment was initiated. The mice received 10 mg/kg oxaliplatin once a week for 3 weeks. Fig. 15*A* shows that administration of oxaliplatin drastically inhibits [^{18}F]-FDG uptake in the $p53^{KO}Cry^{DKO}$ tumor compared to the $p53^{KO}$ tumor. In parallel with this effect on metabolism, oxaliplatin suppressed tumor growth in $p53^{KO}Cry^{DKO}$ but had no measurable effect on the growth rate of the $p53^{KO}$ tumor (Fig. 15*B*).

In vivo measurements of caspase 3 activity of the two groups of tumors after the drug treatment revealed that there was massive apoptosis in the tumor with the $p53^{KO}Cry^{DKO}$ genotype (Fig. 15*C*), which provides a mechanistic explanation of the favorable response to oxaliplatin of tumors of this genotype. Thus, the tumor xenograft study supports the prediction based on apoptosis and toxicity experiments with cultured cells that cryptochrome

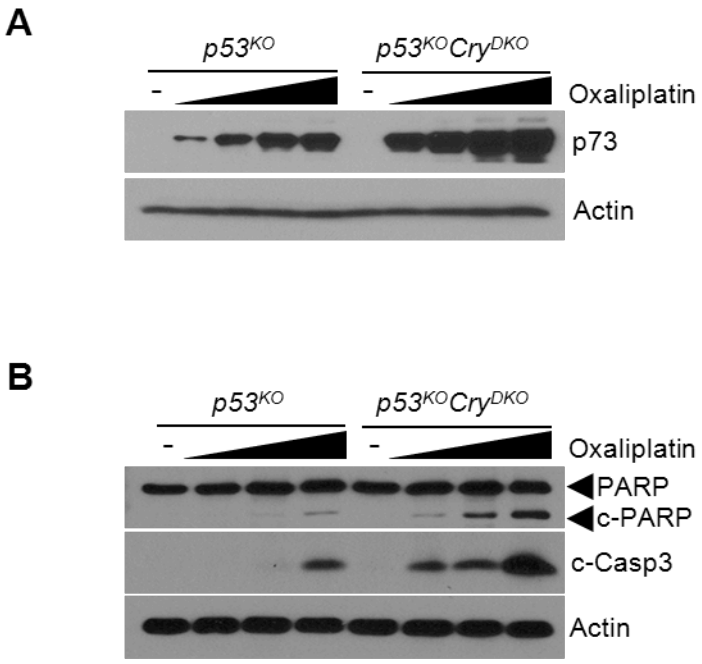
A
p53KO
p53KOCryDKO
-
-
Oxaliplatin
p73
Actin
B
p53KO
p53KOCryDKO
-
-
Oxaliplatin
PARP
c-PARP
c-Casp3
Actin
C
100
80
60
40
20
0
Viability (%)
p53KO
p53KOCryDKO
0
4
8
12
16
20
Oxaliplatin (μM)

Fig. 13. *$p53^{KO}Cry^{DKO}$* cells are more sensitive to oxaliplatin-induced apoptosis and clonogenic killing than *$p53^{KO}$* cells. (A) Induction of p73 by oxaliplatin. Cells of the indicated genotypes were treated with 0,2,5,10, or 20 μM oxaliplatin, harvested 24 hrs later and p73 induction was probed by immunoblotting. (*B*) Cells were treated with 0,5,10, or 20 μM oxaliplatin, harvested 24 hrs later and analyzed for apoptosis by immunoblotting for PARP and caspase 3. (*C*) Clonogenic survival of oxaliplatin treated cells (±s.d., n=3).

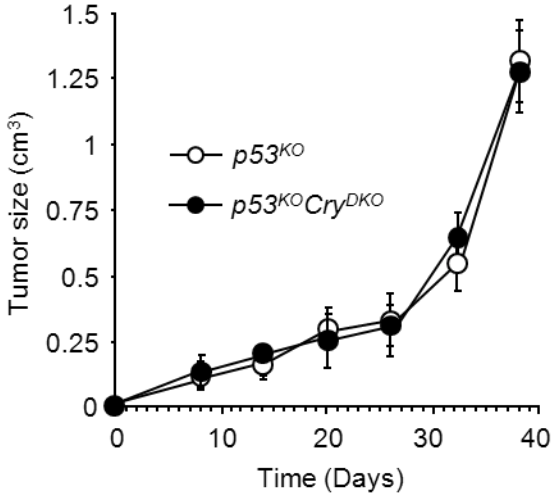

Fig. 14. Growth rates of *p53*^{KO} and *p53*^{KO}*Cry*^{DKO} xenograft in NOD/SCID mice. Tumor xenografts were established by subcutaneous injection of 2×10^6 cells of a *p53*^{KO} genotype on the left flank and a *p53*^{KO}*Cry*^{DKO} genotype on the right flank in a 6-week-old female mouse. Tumor growth was monitored by a caliper and the size is plotted as a function of time after inoculation. The values are means ±s.d. (n=10).

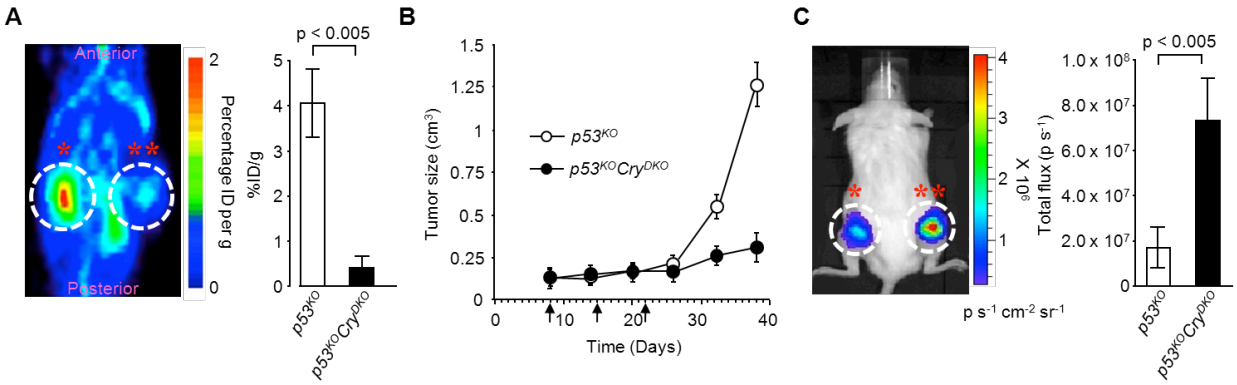
A
Anterior
Posterior
*
**
2
0
Percentage ID per g
p < 0.005
%ID/g
5
4
3
2
1
0
p53KO
p53KOCryDKO
B
Tumor size (cm3)
1.5
1.25
1
0.75
0.5
0.25
0
p53KO
p53KOCryDKO
0
10
20
30
40
Time (Days)
C
4
3
2
1
X 10⁶
p s-1 cm-2 sr-1
p < 0.005
Total flux (p s-1)
1.0 x 10⁸
8.0 x 10⁷
6.0 x 10⁷
4.0 x 10⁷
2.0 x 10⁷
0
p53KO
p53KOCryDKO

Fig. 15. Effect of cryptochrome mutation on treating cancer with p53-null mutation. NOD/SCID mice bearing a $p53^{KO}$ tumor xenograft on the left flank (*) and a $p53^{KO}Cry^{DKO}$ tumor xenograft on the right flank (**) received oxaliplatin intraperitoneally at 10 mg/kg once a week for 21 days and various tumor-related metrics were recorded. (*A*) Tumor metabolism. MicroPET scan recorded 1 hr after [^{18}F]-FDG injection on day 38 after xenograft injection. The right panel shows the quantification of [^{18}F]-FDG signal calculated as the ratio of % injected dose (ID) at region of interest (ROI, circle) to the % ID at a background region. Error bars represent means ±s.d. (n=4). The dorsal aspect is shown. (*B*) Tumor growth. The arrows indicate days of oxaliplatin injection following the xenograft injection on day 0. The oxaliplatin treatment was initiated after tumor size had reached 0.1 cm^3. Error bars represent means ±s.d. (n=10). (*C*) Oxaliplatin-induced apoptosis in xenografts. The NOD/SCID mice were injected with $p53^{KO}$-*Luc* cells in the left flank (*) and $p53^{KO}Cry^{DKO}$-*Luc* cells in the right flank (**). One week later, weekly injections with oxaliplatin were initiated. After the third round of oxaliplatin injection, 2-DEVD-aminoluciferin prosubstrate for caspase 3 was administered i.p. and 10 mins later, bioluminescence was measured in ROI (circle) drawn over the tumor. Quantitative analysis is in the right panel. Error bars represent means ±s.d. (n=4).

disruption in p53-null cells makes them more sensitive to chemotherapy by oxaliplatin.

Conclusion

In Fig. 16, I summarize the findings of this study: *Egr1* is a clock-controlled gene and *p73* is a second order clock-controlled gene which is regulated through Egr1 by the clock and through C-EBPα by the DNA damage response reaction. In the absence of Cry, Egr1 is elevated and upon DNA damage the release of C-EBPα from the *p73* promoter leads to Egr1-activated upregulation of p73 and thus p53-independent apoptosis. These findings suggest that in p53 mutant tumors, which constitute about 50% of all human tumors, targeted inhibition of Cry may improve the efficacy of platinum-based chemotherapy or of combination chemotherapy that includes *cis*-platinum drugs.

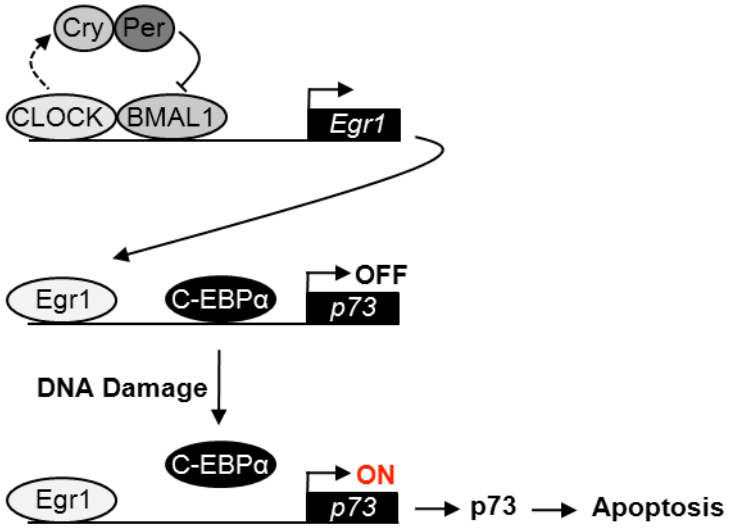

Fig. 16. Model for targeting the clock to improve the efficacy of oxaliplatin treatment of p53-null tumors. Cry regulates Egr1 which transactivates p73. With Cry inactive, Egr1 is upregulated. Following oxaliplatin induced removal of C-EBPα from the *p73* promoter, Egr1 causes massive production of p73 and enhanced apoptosis.

DISCUSSION

A previous report demonstrated that germline disruption of cryptochrome in p53-deficient mice, which are highly tumor prone, increased their tumor-free survival (Ozturk et al., 2009). Notably, this effect was associated with an increase in DNA damage sensitivity of the p53-null and Cry-deficient tumor cells compared with those in p53-deficient tumor cells. These are interesting findings given the crucial role of p53 as a cellular executioner after DNA damage. When cells undergo irreparable DNA damage due to exposure to genotoxic stress such as UV radiation, the p53 protein activates transcription of proapoptotic target genes, effectively removing the damaged cells from the organism. Consequently, loss of p53 in both humans and mice allows cells to persist and acquire new mutations necessary for cancer progression, yielding tumors that are refractory to our most common therapies, including ionizing radiation and chemotherapy. This previous report therefore suggested that loss of cryptochrome could reverse the DNA damage resistance induced by loss of p53. Killing such p53-deficient tumor cells is clearly one of the major challenges in cancer therapy.

The model proposed herein provides insight into the mechanism by which cryptochrome deficiency sensitizes cells lacking p53 to apoptosis. I demonstrated that cryptochrome is involved in the regulation of the p53-related gene *p73*, which like p53 functions as a tumor suppressor and helps maintain genomic integrity (Irwin et al., 2003; Tomasini et al., 2008; Wang et al., 2006). Transcription of p73, strong structural and functional similarity to p53, is enhanced in Cry-deficient cells in response to DNA damage. Loss of cryptochrome relieves repression of Clock/Bmal1, thereby leading to Egr1 up-regulation and recruitment to the *p73* promoter. Activation of p73 after cryptochrome loss

also requires the DNA damage-induced removal of the repressor C-EBPα from the *p73* promoter. Thus, p73 is both temporally regulated by the circadian clock and acutely regulated in response to DNA damage.

These findings may have significant implications in the field of cancer chronotherapy, which seeks to determine whether the effectiveness and tolerability of chemotherapy can be linked to the time of day treatment is given. Indeed, it has been found that treatment schedule can impact both long-term survival and nonspecific toxicity (Hrushesky, 1985; Levi et al., 1990). However, the widespread application of such observations to standard clinical practice has been hampered by a lack of insight into how the circadian cycle influences the response to specific chemotherapeutic agents. I also demonstrated that p53-deficient tumor cells with cryptochrome disruption exhibit increased apoptosis and slower tumor growth *in vivo* after treatment with oxaliplatin. The finding that this effect is linked to p73 supports previous studies showing that platinum agents induce apoptosis at least in part through phosphorylation-dependent activation of p73 (Gong et al., 1999; Leong et al., 2007) and that p73 levels are a key determinant of chemosensitivity (Ibrahim et al., 2010; Irwin et al., 2003). It will therefore be of interest to determine whether the cryptochrome- and p73-dependent response is specific to treatment with platinum or will be seen with other common chemotherapeutic agents.

In addition to enhancing tumor chemosensitivity, these findings might also provide the strategy for approaches to limit the toxicity of chemotherapy for normal tissues. The model proposed herein suggests that in normal cells, the circadian cycling may result in a window when the amount of Egr1 bound to the *p73* promoter is low, potentially blunting the apoptotic response of normal cells to chemotherapy. Interestingly, it has been found that

tumor cells in patients do not cycle with the same kinetics as their normal cells (Klevecz et al., 1987). Thus, an optimal treatment schedule might involve administration of DNA-damaging agents when p73 levels are lowest in normal cells to reduce toxicity but higher in tumor cells to increase sensitivity. Interestingly, the DNA repair protein XPA is elevated in Cry-deficient mouse tissues, and as a result tissues of these mutant mice undergo more efficient nucleotide excision repair in response to cisplatin treatment than wild-type cells (Kang et al., 2010; Kang et al., 2011). Thus, although loss of cryptochromes makes *p53*-deficient tumor cells more sensitive to chemotherapy, the opposite may be true in normal cells. This difference may be explained in part by the fact that in some cellular contexts, p53 can mediate cell cycle arrest and DNA repair as opposed to inducing apoptosis. Thus, therapeutic targeting of cryptochrome function may allow for a coordinate increase in chemosensitivity of tumor cells and decrease in toxicity for normal cells.

The results presented herein demonstrate that $p53^{KO}Cry^{DKO}$ tumors are more responsive to oxaliplatin than $p53^{KO}$ tumors. However, UV and oxaliplatin activate the intrinsic apoptosis pathway that is commonly induced by DNA damaging agents (Hotchkiss et al., 2009), whereas the difference in tumor incidence between the two mouse lines was observed in the absence of any external genotoxic stress. Formally, two biochemical pathways of apoptosis have been defined, extrinsic and intrinsic pathways (Hotchkiss et al., 2009; Tait and Green, 2010). In the mitochondria-independent, extrinsic pathway, a member of the tumor necrosis factor family, such as TNFα, binds to its cognate death receptor in the plasma membrane causing clustering of the receptor and the cytoplasmic adaptor molecules, and as a consequence, dimerization of pro-caspase 8. The latter is activated by autoproteolysis in trans to generate initiator caspase 8, which in turn converts pro-caspase

3 to the executioner caspase 3 that dismantles cellular architecture, destroys some key cellular enzymes, and activates caspase activated DNase (CAD) which attacks chromosomes, generating the apoptosis signature feature, the "nucleosome ladder" (Enari et al., 1998; Sakahira et al., 1998). Of interest, recent work indicates that the core circadian clock participates in the extrinsic pathway by regulating the synthesis of TNFα (Hashiramoto et al., 2010). Moreover, as TNFα is known to be involved in the inflammatory response, Cry^{DKO} mice which overexpress TNFα are uniquely sensitive to inflammatory stimuli and exhibit a rheumatoid arthritis-like syndrome caused by such stimuli (Keller et al., 2009). Thus, it is conceivable that the loss of cryptochrome may amplify the extrinsic pathway for apoptosis to eliminate cells with potential to give rise to cancer. It will therefore be of interest to determine if the clock disruption through cryptochrome inhibition sensitizes the transformed cells to apoptosis by inflammatory cytokines such as TNFα. Clearly, this future study will provide further mechanistic explanations for the reduction of cancer risk in p53-deficient mice by the Cry mutation.

In summary, this study describes a novel circadian clock controlled-apoptotic pathway at a mechanistic level, which drives the induction of apoptosis in p53-deficient cancer cells. Our findings suggest that cryptochrome inhibition may be used as an adjuvant in chemotherapy of p53-null cancer by genotoxic agents such as platinum-based drugs.

REFERENCES

Agami, R., Blandino, G., Oren, M., and Shaul, Y. (1999). Interaction of c-Abl and p73alpha and their collaboration to induce apoptosis. Nature *399*, 809-813.

Bai, L., Zimmer, S., Rickes, O., Rohleder, N., Holthues, H., Engel, L., Leube, R., and Spessert, R. (2008). Daily oscillation of gene expression in the retina is phase-advanced with respect to the pineal gland. Brain Res *1203*, 89-96.

Bell-Pedersen, D., Cassone, V.M., Earnest, D.J., Golden, S.S., Hardin, P.E., Thomas, T.L., and Zoran, M.J. (2005). Circadian rhythms from multiple oscillators: lessons from diverse organisms. Nat Rev Genet *6*, 544-556.

Brautigam, C.A., Smith, B.S., Ma, Z., Palnitkar, M., Tomchick, D.R., Machius, M., and Deisenhofer, J. (2004). Strucutre of the photolyase-like domain of cryptochrome 1 from Arabidopsis thaliana. Proc Natl Acad Sci U S A *101*, 12142-12147.

Cashmore, A.R. (2003). Cryptochromes: enabling plants and animals to determine circadian time. Cell *114*, 537-543.

Cohen, S.J., Cohen, R.B., and Meropol, N.J. (2005). Targeting signal transduction pathways in colorectal cancer--more than skin deep. J Clin Oncol *23*, 5374-5385.

Costanzo, A., Merlo, P., Pediconi, N., Fulco, M., Sartorelli, V., Cole, P.A., Fontemaggi, G., Fanciulli, M., Schiltz, L., Blandino, G.*, et al.* (2002). DNA damage-dependent acetylation of p73 dictates the selective activation of apoptotic target genes. Mol Cell *9*, 175-186.

Danial, N.N., and Korsmeyer, S.J. (2004). Cell death: critical control points. Cell *116*, 205-219.

Enari, M., Sakahira, H., Yokoyama, H., Okawa, K., Iwamatsu, A., and Nagata, S. (1998). A caspase-activated DNase that degrades DNA during apoptosis, and its inhibitor ICAD. Nature *391*, 43-50.

Flores, E.R., Sengupta, S., Miller, J.B., Newman, J.J., Bronson, R., Crowley, D., Yang, A., McKeon, F., and Jacks, T. (2005). Tumor predisposition in mice mutant for p63 and p73: evidence for broader tumor suppressor functions for the p53 family. Cancer Cell *7*, 363-373.

Flores, E.R., Tsai, K.Y., Crowley, D., Sengupta, S., Yang, A., McKeon, F., and Jacks, T. (2002). p63 and p73 are required for p53-dependent apoptosis in response to DNA damage. Nature *416*, 560-564.

Fridman, J.S., and Lowe, S.W. (2003). Control of apoptosis by p53. Oncogene *22*, 9030-9040.

Gallego, M., and Virshup, D.M. (2007). Post-translational modifications regulate the ticking of the circadian clock. Nat Rev Mol Cell Biol *8*, 139-148.

Gauger, M.A., and Sancar, A. (2005). Cryptochrome, circadian cycle, cell cycle checkpoints, and cancer. Cancer Res *65*, 6828-6834.

Gong, J.G., Costanzo, A., Yang, H.Q., Melino, G., Kaelin, W.G., Jr., Levrero, M., and Wang, J.Y. (1999). The tyrosine kinase c-Abl regulates p73 in apoptotic response to cisplatin-induced DNA damage. Nature *399*, 806-809.

Green, C.B., Takahashi, J.S., and Bass, J. (2008). The meter of metabolism. Cell *134*, 728-742.

Grundschober, C., Delaunay, F., Puhlhofer, A., Triqueneaux, G., Laudet, V., Bartfai, T., and Nef, P. (2001). Circadian regulation of diverse gene products revealed by mRNA expression profiling of synchronized fibroblasts. J Biol Chem *276*, 46751-46758.

Hall, J.C. (2000). Cryptochromes: sensory reception, transduction, and clock functions subserving circadian systems. Current opinion in neurobiology *10*, 456-466.

Hashiramoto, A., Yamane, T., Tsumiyama, K., Yoshida, K., Komai, K., Yamada, H., Yamazaki, F., Doi, M., Okamura, H., and Shiozawa, S. (2010). Mammalian clock gene Cryptochrome regulates arthritis via proinflammatory cytokine TNF-alpha. J Immunol *184*, 1560-1565.

Hastings, M.H., Reddy, A.B., and Maywood, E.S. (2003). A clockwork web: circadian timing in brain and periphery, in health and disease. Nat Rev Neurosci *4*, 649-661.

Hollstein, M., Hergenhahn, M., Yang, Q., Bartsch, H., Wang, Z.Q., and Hainaut, P. (1999). New approaches to understanding p53 gene tumor mutation spectra. Mutat Res *431*, 199-209.

Hotchkiss, R.S., Strasser, A., McDunn, J.E., and Swanson, P.E. (2009). Cell death. N Engl J Med *361*, 1570-1583.

Hrushesky, W.J. (1985). Circadian timing of cancer chemotherapy. Science *228*, 73-75.

Hsu, D.S., Zhao, X., Zhao, S., Kazantsev, A., Wang, R.P., Todo, T., Wei, Y.F., and Sancar, A. (1996). Putative human blue-light photoreceptors hCRY1 and hCRY2 are flavoproteins. Biochemistry *35*, 13871-13877.

Humphries, A., and Carter, D.A. (2004). Circadian dependency of nocturnal immediate-early protein induction in rat retina. Biochem Biophys Res Commun *320*, 551-556.

Ibrahim, N., He, L., Leong, C.O., Xing, D., Karlan, B.Y., Swisher, E.M., Rueda, B.R., Orsulic, S., and Ellisen, L.W. (2010). BRCA1-associated epigenetic regulation of p73 mediates an effector pathway for chemosensitivity in ovarian carcinoma. Cancer research *70*, 7155-7165.

Irwin, M., Marin, M.C., Phillips, A.C., Seelan, R.S., Smith, D.I., Liu, W., Flores, E.R., Tsai, K.Y., Jacks, T., Vousden, K.H.*, et al.* (2000). Role for the p53 homologue p73 in E2F-1-induced apoptosis. Nature *407*, 645-648.

Irwin, M.S., and Kaelin, W.G., Jr. (2001). Role of the newer p53 family proteins in malignancy. Apoptosis *6*, 17-29.

Irwin, M.S., Kondo, K., Marin, M.C., Cheng, L.S., Hahn, W.C., and Kaelin, W.G., Jr. (2003). Chemosensitivity linked to p73 function. Cancer Cell *3*, 403-410.

Johnstone, R.W., Ruefli, A.A., and Lowe, S.W. (2002). Apoptosis: a link between cancer genetics and chemotherapy. Cell *108*, 153-164.

Jost, C.A., Marin, M.C., and Kaelin, W.G., Jr. (1997). p73 is a simian [correction of human] p53-related protein that can induce apoptosis. Nature *389*, 191-194.

Jung, Y., and Lippard, S.J. (2007). Direct cellular responses to platinum-induced DNA damage. Chem Rev *107*, 1387-1407.

Junttila, M.R., and Evan, G.I. (2009). p53--a Jack of all trades but master of none. Nat Rev Cancer *9*, 821-829.

Kaghad, M., Bonnet, H., Yang, A., Creancier, L., Biscan, J.C., Valent, A., Minty, A., Chalon, P., Lelias, J.M., Dumont, X.*, et al.* (1997). Monoallelically expressed gene related to p53 at 1p36, a region frequently deleted in neuroblastoma and other human cancers. Cell *90*, 809-819.

Kang, T.H., Lindsey-Boltz, L.A., Reardon, J.T., and Sancar, A. (2010). Circadian control of XPA and excision repair of cisplatin-DNA damage by cryptochrome and HERC2 ubiquitin ligase. Proc Natl Acad Sci U S A *107*, 4890-4895.

Kang, T.H., Reardon, J.T., and Sancar, A. (2011). Regulation of nucleotide excision repair activity by transcriptional and post-transcriptional control of the XPA protein. Nucleic acids research *39*, 3176-3187.

Kelland, L. (2007). The resurgence of platinum-based cancer chemotherapy. Nat Rev Cancer *7*, 573-584.

Keller, M., Mazuch, J., Abraham, U., Eom, G.D., Herzog, E.D., Volk, H.D., Kramer, A., and Maier, B. (2009). A circadian clock in macrophages controls inflammatory immune responses. Proc Natl Acad Sci U S A *106*, 21407-21412.

Klevecz, R.R., Shymko, R.M., Blumenfeld, D., and Braly, P.S. (1987). Circadian gating of S phase in human ovarian cancer. Cancer research *47*, 6267-6271.

Lee, C., Etchegaray, J.P., Cagampang, F.R., Loudon, A.S., and Reppert, S.M. (2001). Posttranslational mechanisms regulate the mammalian circadian clock. Cell *107*, 855-867.

Leong, C.O., Vidnovic, N., DeYoung, M.P., Sgroi, D., and Ellisen, L.W. (2007). The p63/p73 network mediates chemosensitivity to cisplatin in a biologically defined subset of primary breast cancers. J Clin Invest *117*, 1370-1380.

Levi, F., Benavides, M., Chevelle, C., Le Saunier, F., Bailleul, F., Misset, J.L., Regensberg, C., Vannetzel, J.M., Reinberg, A., and Mathe, G. (1990). Chemotherapy of advanced ovarian cancer with 4'-O-tetrahydropyranyl doxorubicin and cisplatin: a randomized phase II trial with an evaluation of circadian timing and dose-intensity. J Clin Oncol *8*, 705-714.

Li, Y.F., Kim, S.T., and Sancar, A. (1993). Evidence for lack of DNA photoreactivating enzyme in humans. Proc Natl Acad Sci U S A *90*, 4389-4393.

Lin, C., Robertson, D.E., Ahmad, M., Raibekas, A.A., Jorns, M.S., Dutton, P.L., and Cashmore, A.R. (1995). Association of flavin adenine dinucleotide with the Arabidopsis blue light receptor CRY1. Science *269*, 968-970.

Lin, C., and Shalitin, D. (2003). Cryptochrome structure and signal transduction. Annual review of plant biology *54*, 469-496.

Lin, K.W., Nam, S.Y., Toh, W.H., Dulloo, I., and Sabapathy, K. (2004). Multiple stress signals induce p73beta accumulation. Neoplasia *6*, 546-557.

Lowe, S.W., Bodis, S., McClatchey, A., Remington, L., Ruley, H.E., Fisher, D.E., Housman, D.E., and Jacks, T. (1994). p53 status and the efficacy of cancer therapy in vivo. Science *266*, 807-810.

Lowe, S.W., Cepero, E., and Evan, G. (2004). Intrinsic tumour suppression. Nature *432*, 307-315.

Lowe, S.W., Ruley, H.E., Jacks, T., and Housman, D.E. (1993). p53-dependent apoptosis modulates the cytotoxicity of anticancer agents. Cell *74*, 957-967.

Lowrey, P.L., and Takahashi, J.S. (2004). Mammalian circadian biology: elucidating genome-wide levels of temporal organization. Annu Rev Genomics Hum Genet *5*, 407-441.

Malhotra, K., Kim, S.T., Batschauer, A., Dawut, L., and Sancar, A. (1995). Putative blue-light photoreceptors from Arabidopsis thaliana and Sinapis alba with a high degree of sequence homology to DNA photolyase contain the two photolyase cofactors but lack DNA repair activity. Biochemistry *34*, 6892-6899.

Marabese, M., Vikhanskaya, F., Rainelli, C., Sakai, T., and Broggini, M. (2003). DNA damage induces transcriptional activation of p73 by removing C-EBPalpha repression on E2F1. Nucleic Acids Res *31*, 6624-6632.

Melino, G., De Laurenzi, V., and Vousden, K.H. (2002). p73: Friend or foe in tumorigenesis. Nat Rev Cancer *2*, 605-615.

Melino, G., Lu, X., Gasco, M., Crook, T., and Knight, R.A. (2003). Functional regulation of p73 and p63: development and cancer. Trends Biochem Sci *28*, 663-670.

Merrow, M., Spoelstra, K., and Roenneberg, T. (2005). The circadian cycle: daily rhythms from behaviour to genes. EMBO Rep *6*, 930-935.

Meulmeester, E., and Jochemsen, A.G. (2008). p53: a guide to apoptosis. Curr Cancer Drug Targets *8*, 87-97.

Mills, A.A., Zheng, B., Wang, X.J., Vogel, H., Roop, D.R., and Bradley, A. (1999). p63 is a p53 homologue required for limb and epidermal morphogenesis. Nature *398*, 708-713.

Miyamoto, Y., and Sancar, A. (1998). Vitamin B2-based blue-light photoreceptors in the retinohypothalamic tract as the photoactive pigments for setting the circadian clock in mammals. Proc Natl Acad Sci U S A *95*, 6097-6102.

Miyamoto, Y., and Sancar, A. (1999). Circadian regulation of cryptochrome genes in the mouse. Brain research Molecular brain research *71*, 238-243.

Munro, A.J., Lain, S., and Lane, D.P. (2005). P53 abnormalities and outcomes in colorectal cancer: a systematic review. Br J Cancer *92*, 434-444.

Ozgur, S., and Sancar, A. (2003). Purification and properties of human blue-light photoreceptor cryptochrome 2. Biochemistry *42*, 2926-2932.

Ozturk, N., Lee, J.H., Gaddameedhi, S., and Sancar, A. (2009). Loss of cryptochrome reduces cancer risk in p53 mutant mice. Proc Natl Acad Sci U S A *106*, 2841-2846.

Panda, S., Antoch, M.P., Miller, B.H., Su, A.I., Schook, A.B., Straume, M., Schultz, P.G., Kay, S.A., Takahashi, J.S., and Hogenesch, J.B. (2002). Coordinated transcription of key pathways in the mouse by the circadian clock. Cell *109*, 307-320.

Partch, C.L., Clarkson, M.W., Ozgur, S., Lee, A.L., and Sancar, A. (2005). Role of structural plasticity in signal transduction by the cryptochrome blue-light photoreceptor. Biochemistry *44*, 3795-3805.

Partch, C.L., and Sancar, A. (2005). Photochemistry and photobiology of cryptochrome blue-light photopigments: the search for a photocycle. Photochemistry and photobiology *81*, 1291-1304.

Preitner, N., Damiola, F., Lopez-Molina, L., Zakany, J., Duboule, D., Albrecht, U., and Schibler, U. (2002). The orphan nuclear receptor REV-ERBalpha controls circadian transcription within the positive limb of the mammalian circadian oscillator. Cell *110*, 251-260.

Reppert, S.M., and Weaver, D.R. (2002). Coordination of circadian timing in mammals. Nature *418*, 935-941.

Roos, W., Baumgartner, M., and Kaina, B. (2004). Apoptosis triggered by DNA damage O6-methylguanine in human lymphocytes requires DNA replication and is mediated by p53 and Fas/CD95/Apo-1. Oncogene *23*, 359-367.

Sahar, S., and Sassone-Corsi, P. (2009). Metabolism and cancer: the circadian clock connection. Nat Rev Cancer *9*, 886-896.

Sakahira, H., Enari, M., and Nagata, S. (1998). Cleavage of CAD inhibitor in CAD activation and DNA degradation during apoptosis. Nature *391*, 96-99.

Sancar, A. (2000). Cryptochrome: the second photoactive pigment in the eye and its role in circadian photoreception. Annual review of biochemistry *69*, 31-67.

Sancar, A. (2003). Structure and function of DNA photolyase and cryptochrome blue-light photoreceptors. Chemical reviews *103*, 2203-2237.

Sancar, A. (2004a). Photolyase and cryptochrome blue-light photoreceptors. Advances in protein chemistry *69*, 73-100.

Sancar, A. (2004b). Regulation of the mammalian circadian clock by cryptochrome. The Journal of biological chemistry *279*, 34079-34082.

Sancar, A. (2008). The intelligent clock and the Rube Goldberg clock. Nature structural & molecular biology *15*, 23-24.

Sato, T.K., Panda, S., Miraglia, L.J., Reyes, T.M., Rudic, R.D., McNamara, P., Naik, K.A., FitzGerald, G.A., Kay, S.A., and Hogenesch, J.B. (2004). A functional genomics strategy reveals Rora as a component of the mammalian circadian clock. Neuron *43*, 527-537.

Schibler, U., and Sassone-Corsi, P. (2002). A web of circadian pacemakers. Cell *111*, 919-922.

Schmitt, C.A., Fridman, J.S., Yang, M., Baranov, E., Hoffman, R.M., and Lowe, S.W. (2002). Dissecting p53 tumor suppressor functions in vivo. Cancer Cell *1*, 289-298.

Stiewe, T. (2007). The p53 family in differentiation and tumorigenesis. Nat Rev Cancer *7*, 165-168.

Stiewe, T., and Putzer, B.M. (2000). Role of the p53-homologue p73 in E2F1-induced apoptosis. Nat Genet *26*, 464-469.

Storch, K.F., Lipan, O., Leykin, I., Viswanathan, N., Davis, F.C., Wong, W.H., and Weitz, C.J. (2002). Extensive and divergent circadian gene expression in liver and heart. Nature *417*, 78-83.

Symonds, H., Krall, L., Remington, L., Saenz-Robles, M., Lowe, S., Jacks, T., and Van Dyke, T. (1994). p53-dependent apoptosis suppresses tumor growth and progression in vivo. Cell *78*, 703-711.

Tait, S.W., and Green, D.R. (2010). Mitochondria and cell death: outer membrane permeabilization and beyond. Nat Rev Mol Cell Biol *11*, 621-632.

Takahashi, J.S., Hong, H.K., Ko, C.H., and McDearmon, E.L. (2008). The genetics of mammalian circadian order and disorder: implications for physiology and disease. Nat Rev Genet *9*, 764-775.

Thompson, C.L., Bowes Rickman, C., Shaw, S.J., Ebright, J.N., Kelly, U., Sancar, A., and Rickman, D.W. (2003). Expression of the blue-light receptor cryptochrome in the human retina. Investigative ophthalmology & visual science *44*, 4515-4521.

Thresher, R.J., Vitaterna, M.H., Miyamoto, Y., Kazantsev, A., Hsu, D.S., Petit, C., Selby, C.P., Dawut, L., Smithies, O., Takahashi, J.S.*, et al.* (1998). Role of mouse cryptochrome blue-light photoreceptor in circadian photoresponses. Science *282*, 1490-1494.

Todo, T. (1999). Functional diversity of the DNA photolyase/blue light receptor family. Mutat Res *434*, 89-97.

Todo, T., Ryo, H., Yamamoto, K., Toh, H., Inui, T., Ayaki, H., Nomura, T., and Ikenaga, M. (1996). Similarity among the Drosophila (6-4)photolyase, a human photolyase homolog, and the DNA photolyase-blue-light photoreceptor family. Science *272*, 109-112.

Tomasini, R., Tsuchihara, K., Wilhelm, M., Fujitani, M., Rufini, A., Cheung, C.C., Khan, F., Itie-Youten, A., Wakeham, A., Tsao, M.S.*, et al.* (2008). TAp73 knockout shows genomic instability with infertility and tumor suppressor functions. Genes Dev *22*, 2677-2691.

Urist, M., and Prives, C. (2002). p53 leans on its siblings. Cancer Cell *1*, 311-313.

van der Horst, G.T., Muijtjens, M., Kobayashi, K., Takano, R., Kanno, S., Takao, M., de Wit, J., Verkerk, A., Eker, A.P., van Leenen, D.*, et al.* (1999). Mammalian Cry1 and Cry2 are essential for maintenance of circadian rhythms. Nature *398*, 627-630.

Vitaterna, M.H., Selby, C.P., Todo, T., Niwa, H., Thompson, C., Fruechte, E.M., Hitomi, K., Thresher, R.J., Ishikawa, T., Miyazaki, J.*, et al.* (1999). Differential regulation of mammalian period genes and circadian rhythmicity by cryptochromes 1 and 2. Proc Natl Acad Sci U S A *96*, 12114-12119.

Vogelstein, B., Lane, D., and Levine, A.J. (2000). Surfing the p53 network. Nature *408*, 307-310.

Wang, W., Kim, S.H., and El-Deiry, W.S. (2006). Small-molecule modulators of p53 family signaling and antitumor effects in p53-deficient human colon tumor xenografts. Proc Natl Acad Sci U S A *103*, 11003-11008.

Yang, A., Kaghad, M., Caput, D., and McKeon, F. (2002). On the shoulders of giants: p63, p73 and the rise of p53. Trends Genet *18*, 90-95.

Yang, A., Kaghad, M., Wang, Y., Gillett, E., Fleming, M.D., Dotsch, V., Andrews, N.C., Caput, D., and McKeon, F. (1998). p63, a p53 homolog at 3q27-29, encodes multiple products with transactivating, death-inducing, and dominant-negative activities. Mol Cell *2*, 305-316.

Yang, A., Schweitzer, R., Sun, D., Kaghad, M., Walker, N., Bronson, R.T., Tabin, C., Sharpe, A., Caput, D., Crum, C.*, et al.* (1999). p63 is essential for regenerative proliferation in limb, craniofacial and epithelial development. Nature *398*, 714-718.

Yang, A., Walker, N., Bronson, R., Kaghad, M., Oosterwegel, M., Bonnin, J., Vagner, C., Bonnet, H., Dikkes, P., Sharpe, A.*, et al.* (2000). p73-deficient mice have neurological, pheromonal and inflammatory defects but lack spontaneous tumours. Nature *404*, 99-103.

Young, M.W., and Kay, S.A. (2001). Time zones: a comparative genetics of circadian clocks. Nat Rev Genet *2*, 702-715.

Yu, J., Baron, V., Mercola, D., Mustelin, T., and Adamson, E.D. (2007). A network of p73, p53 and Egr1 is required for efficient apoptosis in tumor cells. Cell Death Differ *14*, 436-446.

Yuan, Z.M., Shioya, H., Ishiko, T., Sun, X., Gu, J., Huang, Y.Y., Lu, H., Kharbanda, S., Weichselbaum, R., and Kufe, D. (1999). p73 is regulated by tyrosine kinase c-Abl in the apoptotic response to DNA damage. Nature *399*, 814-817.